Chem Soc Rev

REVIEW ARTICLE

View Article Online
View Journal | View Issue

Check for updates

Cite this: *Chem. Soc. Rev.*, 2025, **54**, 6807

Recent advances in the efficient synthesis of steroid natural products: emerging methods and strategies

Yu Wang and Jinghan Gui *

Steroid natural products (SNPs) play an indispensable role in drug discovery owing to their remarkable structural features and biological activities. However, the inadequate amounts of steroid samples derived from natural sources has limited thorough assessment of SNP bioactivities. Accordingly, chemical synthesis of these compounds has become an important, practical way to obtain them in sufficient quantities. Chemists have been focusing on efficient synthesis of SNPs since the 1930s, and significant breakthroughs have been achieved in the past few decades. This review presents advances in this field over the past 20 years, highlighting key C–C bond formation and reorganization reactions in the construction of steroidal skeletons, as well as redox-relay events for the installation of complex oxidation states. We hope this review will serve as a timely reference to allow researchers to quickly learn about state-of-the-art achievements in SNP synthesis and will inspire the development of more powerful strategies for natural product synthesis.

Received 29th January 2025

DOI: 10.1039/d3cs01150j

rsc.li/chem-soc-rev

Open Access Article. Published on 11 June 2025. Downloaded on 2/11/2026 11:18:29 AM. This article is licensed under a Creative Commons Attribution-NonCommercial 3.0 Unported Licence.

1. Introduction

Because of the scaffold diversity, structural complexity, and varied biological activities of natural products, they have long been targets pursued by synthetic and medicinal chemists.[1] Natural products and their analogues are sources of therapeutic agents for various life-threatening diseases, including cancers, cardiovascular and cerebrovascular diseases, gastrointestinal diseases, central nervous system disorders, and immunological diseases.[2] Natural product synthesis remains among the most exciting and challenging areas of organic chemistry.[3] Newly developed synthetic methods and strategies have enabled significant progress in natural product synthesis, and the complex molecular architectures of natural products have motivated chemists to develop powerful new transformations, thus advancing organic chemistry.[4]

State Key Laboratory of Chemical Biology, Shanghai Institute of Organic Chemistry, University of Chinese Academy of Sciences, Chinese Academy of Sciences, 345 Lingling Road, Shanghai 200032, China. E-mail: guijh@sioc.ac.cn; Web: https://guigroup.sioc.ac.cn

Yu Wang

Yu Wang received his BS degree from Yangzhou University in 2015, and his PhD degree from Shanghai Institute of Organic Chemistry (SIOC) in 2020 under the supervision of Prof. Jinghan Gui. From 2020 to 2021, he was a research associate in the same group. In 2021, he moved to Scripps Research and began his postdoctoral studies with Prof. Phil S. Baran. His research interests mainly focus on synthesis of bioactive complex natural products and invention of novel reagents for organic synthesis.

Jinghan Gui

Jinghan Gui received his BS degree from Anhui Normal University in 2007. After completing his PhD degree at Shanghai Institute of Organic Chemistry (SIOC) under the guidance of Prof. Weisheng Tian in 2012, he went on to pursue his postdoctoral research with Prof. Phil S. Baran at Scripps Research in February 2013. In March 2016, he moved back to SIOC to begin his independent research career. His research focuses on the efficient synthesis of biologically active steroid and terpenoid natural products, and the development of new synthetic methodologies.

Open Access Article. Published on 11 June 2025. Downloaded on 2/11/2026 11:18:29 AM.
This article is licensed under a Creative Commons Attribution-NonCommercial 3.0 Unported Licence.

Steroid natural products (SNPs) are found in a wide range of animals, plants, and microorganisms. SNPs and their analogues are valuable chemical resources with applications in medicine, agrochemistry, and the cosmetics industry, with examples including dexamethasone, brassinolide, and β-sitosterol. As reported in a chart by the Njardarson group at the University of Arizona, steroid-related compounds accounted for 13 of the top 200 small-molecule drugs by retail sales in 2024.[5] Therefore, research on steroid chemistry has attracted significant attention in the field of organic chemistry, which can be traced back to the 18th century. In 1758, French physician François Poulletier de la Salle was the first to isolate crystalline cholesterol from gallstones.[6] However, the correct structure of cholesterol was not elucidated until 1933. Notably, extensive research on the structural elucidation, biosynthesis, chemical synthesis, and molecular regulation of steroids has led to the awarding of several Nobel Prizes. For example, German chemist Heinrich Wieland received the Nobel Prize in Chemistry in 1927 for his investigations into the constitution of bile acids and related compounds. Later, American chemist Robert Burns Woodward was awarded the Nobel Prize in Chemistry in 1965 for his outstanding contributions to the field of organic synthesis, including the total syntheses of cholesterol and cortisone.[7]

Classical steroids are characterized by a 6/6/6/5 tetracyclic skeleton, and their isolation, structural elucidation, chemical synthesis, and biogenetic origins[8] have been widely studied, starting in the twentieth century (Fig. 1(A)). Rearranged steroids, which are biosynthetically generated from classical

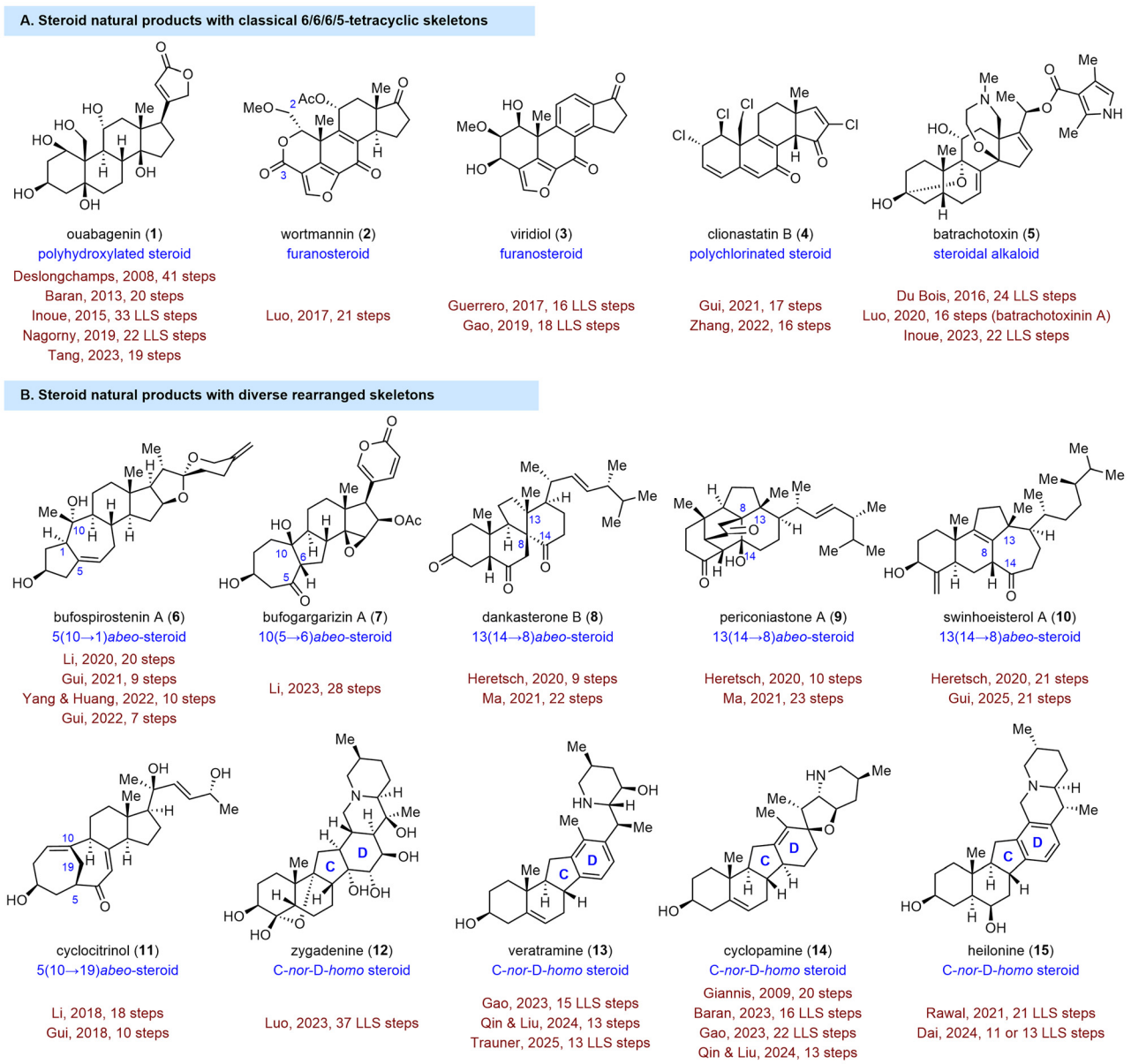

Fig. 1 Selected steroid natural products (SNPs) with classical and rearranged skeletons. (A) Selected steroids that possess classical 6/6/6/5-tetracyclic skeletons; (B) Selected steroids that possess diverse rearranged skeletons.

 This journal is © The Royal Society of Chemistry 2025

Open Access Article. Published on 11 June 2025. Downloaded on 2/11/2026 11:18:29 AM.
This article is licensed under a Creative Commons Attribution-NonCommercial 3.0 Unported Licence.

steroids through one or more C–C bond migrations and scissions (Fig. 1(B)), have garnered increasing attention from synthetic chemists over the last two decades.[9] Despite the structural complexity of SNPs, the past 20 years have witnessed tremendous achievements in their efficient synthesis, and thus a systematic review of these achievements is of significant importance. We hope this review will not only be a useful resource for researchers to quickly learn about the state-of-the-art achievements in SNP synthesis but also will stimulate the development of additional novel and efficient synthetic methods and strategies. Owing to limited space, some steroid and triterpenoid syntheses, such as List's synthesis of estrone,[10] Lopchuk's synthesis of withanolides,[11] our group's syntheses of aspersteroids[12] and phomarol,[13] Li's synthesis of phomarol,[14] Dong's synthesis of phainanoid A,[15] Micalizio's synthesis of octanorcucurbitacin B,[16] as well as those that have been included in previous reviews,[9,17] are not covered here.

As summarized in Scheme 1, this review comprises two sections: one for SNPs constructed *via* convergent strategies, and the other for SNPs constructed *via* semisynthetic strategies. Convergent strategies typically require diastereoselective preparation of fragments, followed by convergent union of the fragments and intramolecular cyclization to build the polycyclic framework.[18] Depending on where the key fragment-coupling and cyclization reactions take place (*i.e.*, the A/B, B, C, or D ring), the first section of the review is divided into four subsections (Scheme 1, left). Semisynthetic strategies feature the utilization of inexpensive commercially available steroids, such as pregnenolone ($0.32 per gram) as starting materials (Scheme 1, right).[19] Although these strategies benefit from the utilization of steroidal materials that have tetracyclic frameworks and some of the necessary stereogenic centers, successful implementation of these strategies necessitates precise installation of the requisite oxidation states within the aliphatic core skeleton and controllable skeletal reorganization to quickly forge the rearranged skeleton.[17d,20]

2. Synthesis of SNPs *via* convergent strategies

Convergent strategies have been widely applied to the synthesis of SNPs and have served as crucial tools for increasing synthetic efficiency. Convergent strategies typically involve assembly of two fragments, followed by cyclization and further functionalization to access the target molecules. Because the coupling fragments can be highly functionalized, these strategies often lead to synthetic routes that are shorter than those that rely on linear strategies, wherein the rings are constructed in a stepwise manner. Therefore, reactions that can couple fragments chemo-, regio-, and diastereoselectively become highly appealing. In this section, examples of such reactions are categorized and summarized on the basis of the specific rings (A/B, B, C, or D) that are formed during the key steps (Scheme 2).

2.1. Convergent assembly of the A/B ring system

Strategic bond disconnection at the A/B ring system *via* a cycloaddition can markedly simplify the polycyclic skeleton of an SNP, leading to a simple intermediate that possesses the C/D ring system and can be derived from known chiral pool molecules, such as (+)-Hajos–Parrish ketone and sitolactone.[21] Li's synthesis of bufospirostenin A *via* an alkoxyallene-yne Pauson–Khand reaction to construct the 5/7 bicyclic A/B ring system,[22] and their synthesis of bufogargarizin A by means of a Ru-catalyzed [5+2] cycloaddition to install the 7/5 bicyclic system, have been selected as representative examples (Scheme 3).[23]

2.1.1. Li's synthesis of bufospirostenin A. The 5(10 → 1)-*abeo*-steroid bufospirostenin A (**6**) was isolated by Ye and co-workers in 2017 from the bile of the toad *Bufo bufo gargarizans*.[24] The molecule features a unique 5/7/6/5/5/6 hexacyclic skeleton decorated with 11 stereocenters, as well as a spiroketal E/F ring system. Bufospirostenin A shows 43% inhibitory activity toward Na/K ATPase at 25 μM. The mesmerizing structure of **6** and its promising biological activity have garnered

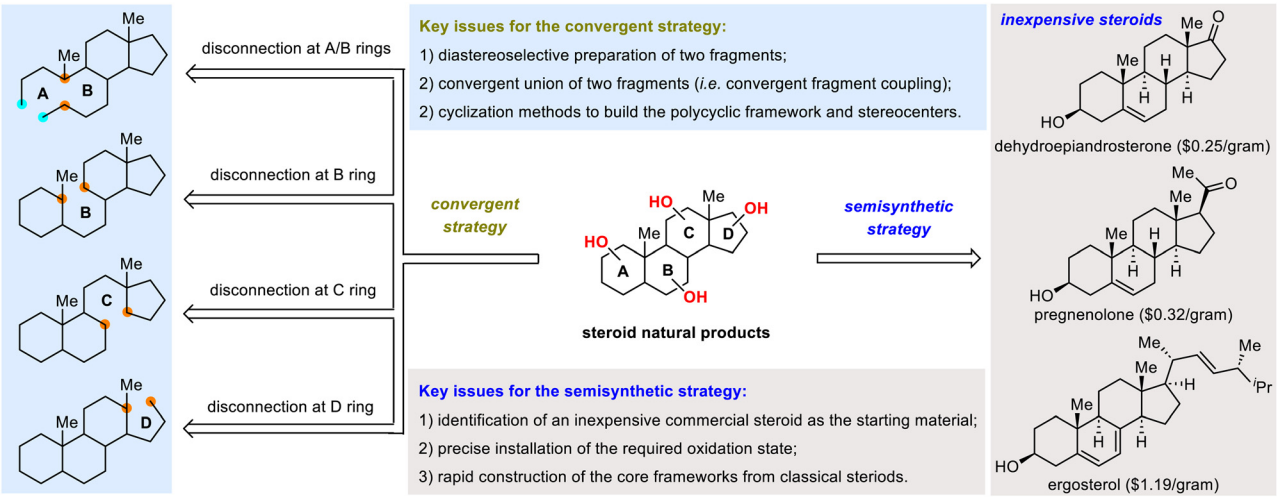

Scheme 1 Convergent and semisynthetic strategies for the synthesis of SNPs.

Open Access Article. Published on 11 June 2025. Downloaded on 2/11/2026 11:18:29 AM.
This article is licensed under a Creative Commons Attribution-NonCommercial 3.0 Unported Licence.

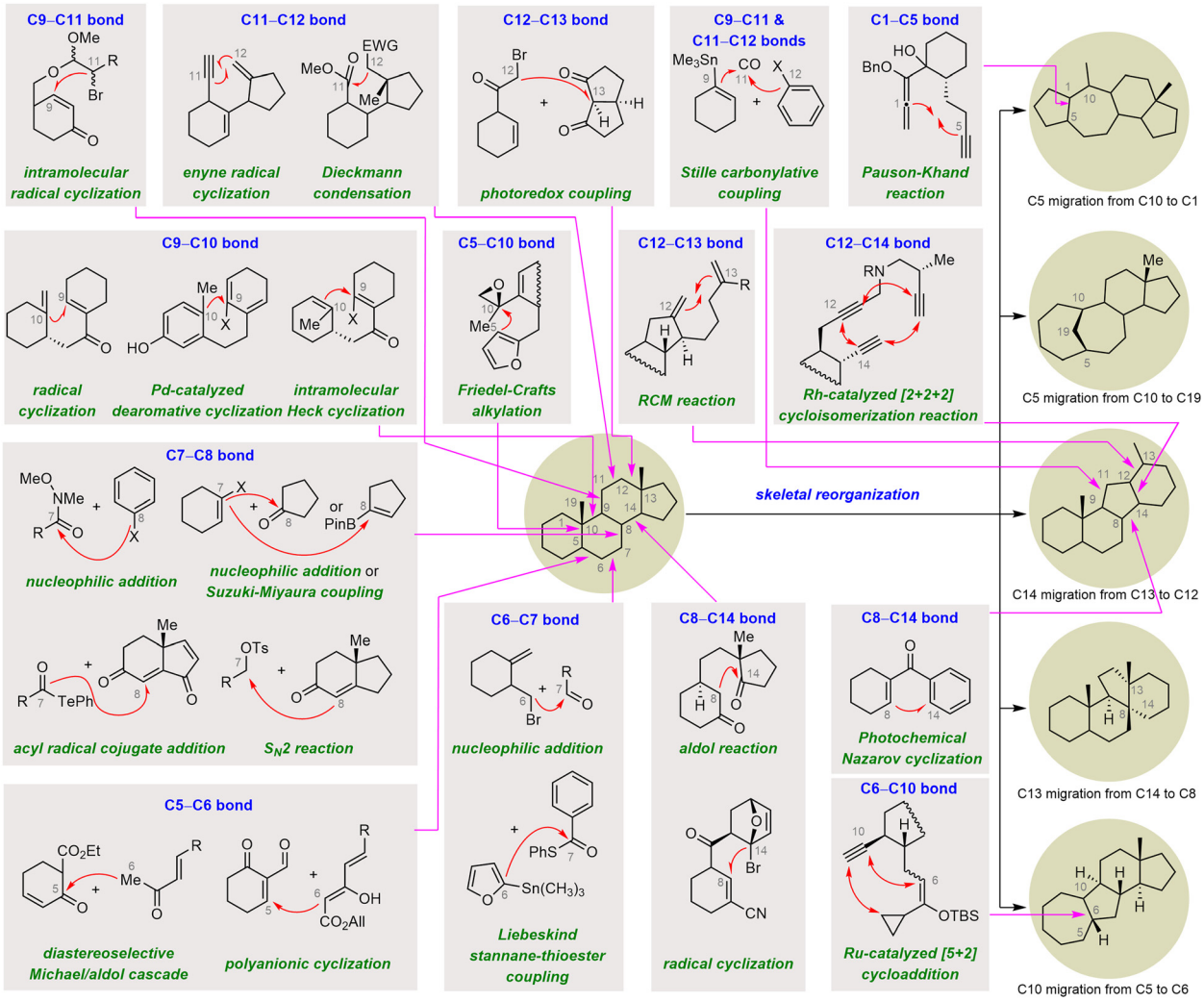

Scheme 2 Strategic bond-forming reactions for efficient synthesis of SNPs.

considerable attention from our group[25] and the groups of Li[22] and Yang[26] between 2020 and 2022. In 2020, Li and co-workers reported the first asymmetric total synthesis of **6**, in which the rearranged A/B ring system was constructed *via* a rhodium-catalyzed Pauson–Khand reaction of an alkoxyallene-yne.[22]

Li's total synthesis commenced with the preparation of alkyne **17** in four steps from **16** (Scheme 4). A nucleophilic addition reaction between the ketone of **17** and an allene lithium reagent derived from **18** and *n*-butyllithium (^{n}BuLi) delivered alkoxyallene-yne **19**, setting the stage for the key intramolecular Pauson–Khand reaction.[27] Extensive optimization experiments revealed that $[RhCl(CO)_2]_2$ was the optimal catalyst, and the reaction was run under a balloon of CO, giving rise to dienone **20**, which has the desired A/B ring system. This compound was transformed into ketone **21** in seven steps, and the E ring of **22** was established in another five steps. Finally, the spiroketal moiety was installed *via* reaction of the lactone with a lithium reagent derived from iodide **23**, followed by acid-promoted spiroketalization, completing the total synthesis of bufospirostenin A.

2.1.2. Li's syntheses of bufogargarizins A and B. Li's syntheses of bufogargarizins A (**7**) and B (**35**) involved another elegant application of an intramolecular cycloaddition for the construction of the A/B ring system. Bufogargarizins A and B are twin 19-*nor*-*abeo*-steroids with rearranged A/B ring systems. They were isolated from the venom of *Bufo bufo gargarizans* in 2010 by Ye and co-workers.[28] Biosynthetically, these *abeo*-steroids are proposed to be derived from the same diketone precursor *via* two different intramolecular aldol condensation pathways.

Central to Li's strategy was a ruthenium-catalyzed [5+2] cycloaddition reaction (Scheme 5).[23] The synthesis started with the preparation of alkyne **25** in nine steps from sitolactone (**24**). Treatment of **25** with trimethylsilyl trifluoromethanesulfonate (TMSOTf) generated silyl enol ether **26**. Crude **26** was subjected to the desired [5+2] cycloaddition reaction catalyzed by CpRu-$(CH_3CN)_3PF_6$ to yield **27**, which possesses the tetracyclic skeleton of bufogargarizin A.[29] Mukaiyama hydration of **27** produced alcohol **28**, which was converted to enol triflate **29** in eight steps. Suzuki coupling of **29** with **30** provided **31**, which was elaborated to bufogargarizin A (**7**) in seven steps.

 This journal is © The Royal Society of Chemistry 2025

Open Access Article. Published on 11 June 2025. Downloaded on 2/11/2026 11:18:29 AM.
This article is licensed under a Creative Commons Attribution-NonCommercial 3.0 Unported Licence.

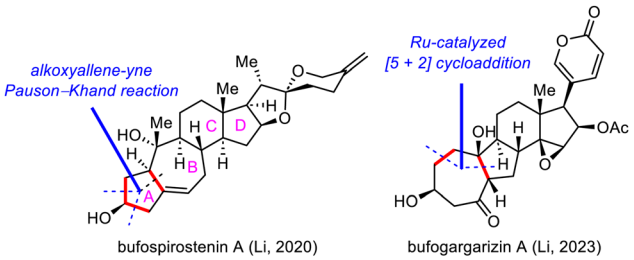

Scheme 3 Retrosynthetic disconnections at the A/B ring system.

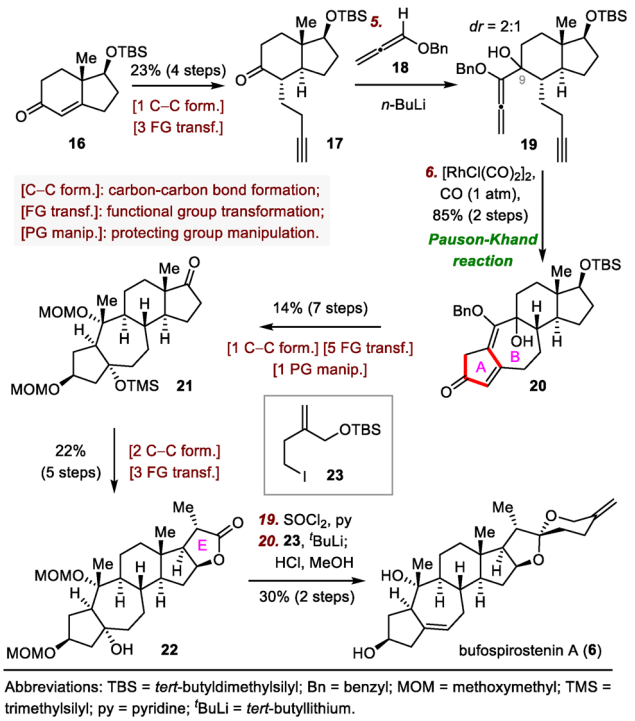

Scheme 4 Li's synthesis of bufospirostenin A (**6**).

Li and co-workers then attempted a direct, bioinspired preparation of bufogargarizin B (**35**) from bufogargarizin A but were unable to accomplish this ideal transformation, despite many attempts; in most cases, undesired byproducts or decomposition of **7** were observed. Eventually, these investigators identified alcohol **32**, which was prepared in four steps from intermediate **28**, as a suitable intermediate for accessing bufogargarizin B *via* a retro-aldol/transannular aldol cascade. Specifically, heating a solution of **32** in tetrahydrofuran (THF) in the presence of 1,8-diazabicyclo[5.4.0]undec-7-ene (DBU) as a base triggered the desired retro-aldol reaction to afford anionic intermediate **33**, which then underwent a transannular aldol reaction to produce ketone **34** in 73% yield. Notably, the entire sequence (**32** → **34**) was completely diastereoselective, an outcome that was supported by density functional theory calculations. The total synthesis of bufogargarizin B was then accomplished in fourteen steps from **34** by means of a route similar to that used for bufogargarizin A. Li *et al.* were unable to directly transform bufogargarizin B into bufogargarizin A.

2.2. Convergent assembly of the B ring

Strategic bond disconnection at the B ring leads to A-ring and C/D-ring fragments of similar structural complexity, thereby maximizing synthetic convergency and shortening the longest linear sequence of steps. Therefore, this disconnection is the one most often used by synthetic chemists. In this subsection of the review, representative work on building the B ring and associated stereogenic centers is described, and key bond-forming reactions are highlighted (Scheme 6).

2.2.1. Deslongchamps's synthesis of ouabagenin. Ouabain, and its aglycone ouabagenin (**1**), are highly oxidized steroids that belong to the cardenolide family, members of which have potential application as Na^+/K^+-ATPase inhibitors.[30] Several family members have been used to treat various cardiac diseases. In 1942, Mannich and Siewert isolated ouabagenin as its monoacetonide by means of hydrochloric acid–promoted hydrolysis of ouabain in acetone.[31] Structurally, ouabagenin possesses a rare highly oxygenated 6/6/6/5 tetracyclic ring system, in which the A/B and C/D ring systems are *cis*-fused, along with a β-oriented butenolide side chain. The interesting biological activity profile and structural complexity of ouabagenin have attracted significant attention from synthetic chemists over the past decades. To date, five syntheses have been reported, including one semisynthesis (by Baran's group[32]) and four total syntheses (by the groups of Deslongchamps,[33] Inoue,[34] Nagorny,[35] and Tang[36]).

In 2008, Deslongchamps and co-workers completed the first total synthesis of ouabagenin by employing a polyanionic cyclization as the key skeletal construction step (Scheme 7).[33] Their synthesis began with a diastereoselective double Michael addition reaction between Nazarov reagent **36** and chiral cyclohexenone **37** in the presence of Cs_2CO_3,[37] which was followed by decarboxylation with $Pd(PPh_3)_4$ to provide aldehyde **38** with the desired *cis*-A/B ring junction. From intermediate **39**, which was prepared from **38** in two steps, the C ring of ouabagenin was forged by means of a classical aldol condensation in the presence of potassium bis(trimethylsilyl)amide (KHMDS), a reaction that delivered key tetracyclic intermediate **40** in 83% yield. Finally, the butenolide side ring was installed *via* treatment of α-hydroxyketone **42** with $Ph_3P{=}C{=}C{=}O$, affording ouabagenin (**1**) after hydrolysis of the four ester groups.

2.2.2. Nagorny's synthesis of ouabagenin. In 2019, Nagorny and co-workers disclosed a total synthesis of ouabagenin that also hinged mainly on a bond disconnection at the B ring.[35] Their synthesis capitalized on a copper(II)-catalyzed diastereoselective Michael/aldol cascade reaction developed by their group in 2015.[38] In addition, this expedient methodology allowed the group to synthesize other cardiotonic steroids, such as 19-hydroxysarmentogenin,[39] trewianin aglycone,[39] and cannogenol-3-*O*-α-l-rhamnoside.[40]

As shown in Scheme 8, the synthesis of ouabagenin commenced with a copper(II)-catalyzed diastereoselective Michael/aldol cascade reaction between enone **43** and β-ketoester **44**,

Open Access Article. Published on 11 June 2025. Downloaded on 2/11/2026 11:18:29 AM.
This article is licensed under a Creative Commons Attribution-NonCommercial 3.0 Unported Licence.

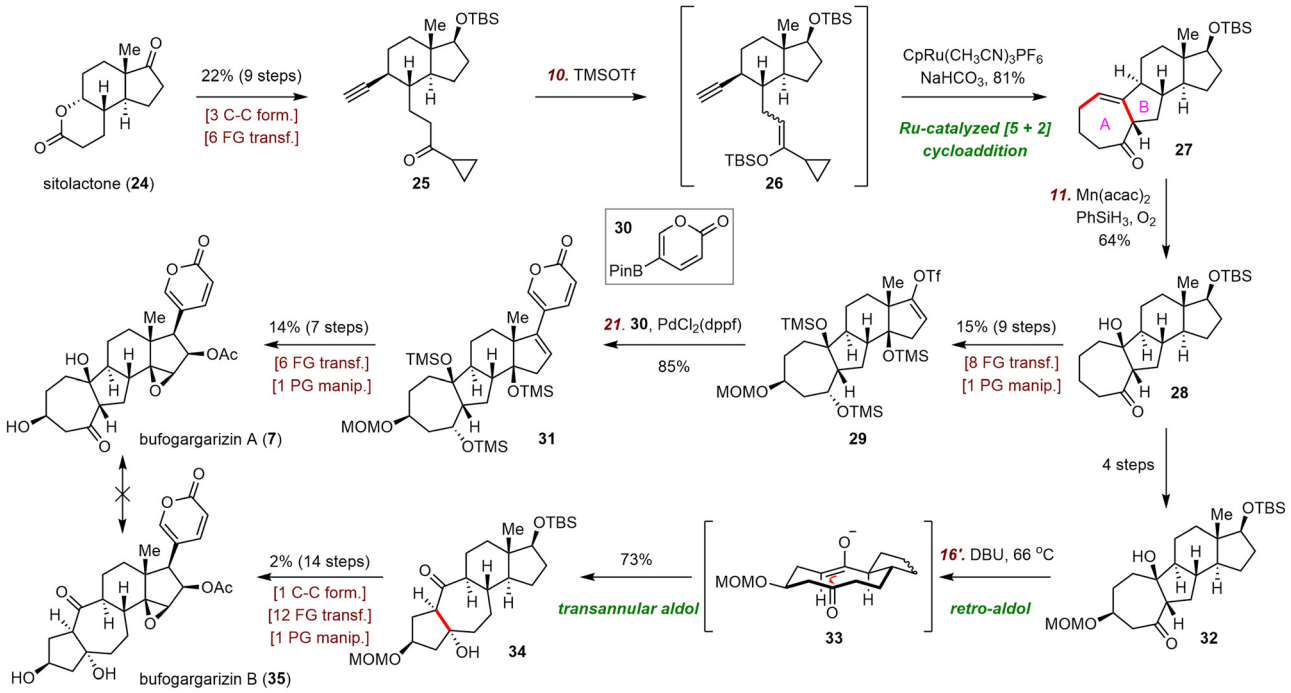

Abbreviations: TMSOTf = trimethylsilyl trifluoromethanesulfonate; acac = acetylacetonyl; $PhSiH_3$ = phenylsilane; Tf = trifluoromethanesulfonyl; Ac = acetyl; dppf = 1,1'-*bis*(diphenylphosphino)ferrocene; DBU = 1,8-diazabicyclo[5.4.0]undec-7-ene.

Scheme 5 Li's syntheses of bufogargarizins A (**7**) and B (**35**).

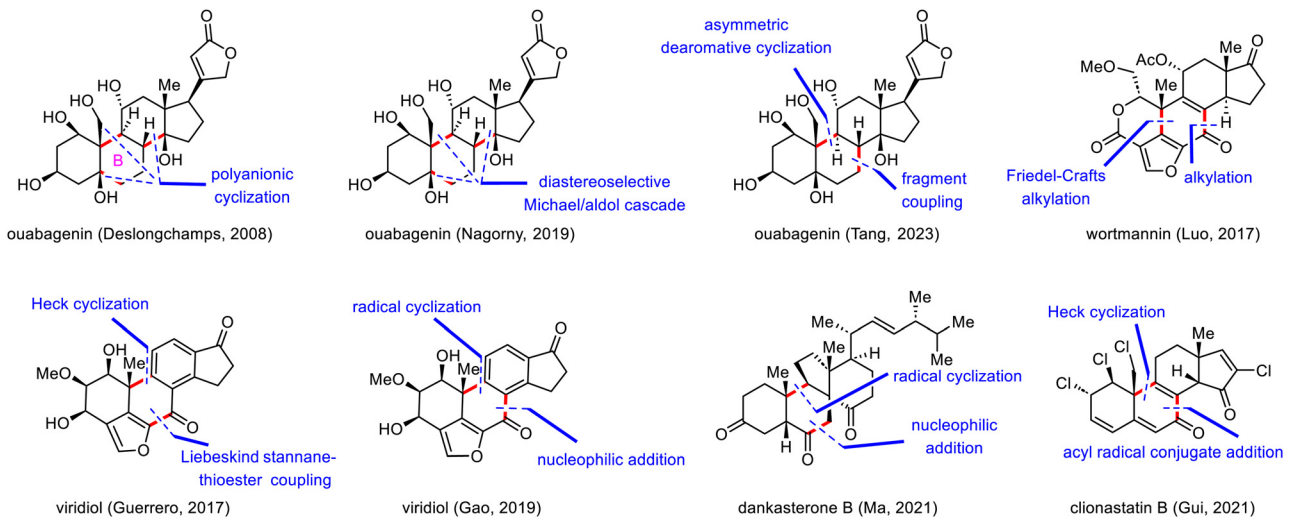

Scheme 6 Retrosynthetic disconnections at the B ring.

affording dienone **45** in 45% yield.[35] After extensive optimization of the reaction parameters, β-hydroxy ketone **45** was eventually isomerized into **46** by treatment with sodium bis(trimethylsilyl)-amide (NaHMDS) in toluene, possibly by means of a retro-aldol/intramolecular aldol cascade reaction. Reduction of **46** with diisobutylaluminium hydride (DIBAL-H) led to an allylic alcohol intermediate, which, upon treatment with aqueous HCO_2H, spontaneously isomerized to produce dienone **47** in 72% yield. Finally, ouabagenin was synthesized in an additional sixteen steps *via* intermediate **48**.

2.2.3. Tang's synthesis of ouabagenin. In 2023, Tang and co-workers reported another total synthesis of ouabagenin, which was achieved by means of an unsaturation-functionalization strategy (Scheme 9).[36] During their synthesis, the tetracyclic skeleton of ouabagenin was efficiently constructed *via* a palladium-catalyzed enantioselective dearomative cyclization reaction,[41] which simultaneously secured the desired stereochemistry at C10.

The synthesis began with an S_N2 reaction of enone **49** with tosylate **50** to afford a coupling product (not shown) that was subjected to triflation and selective removal of the

 This journal is © The Royal Society of Chemistry 2025

Open Access Article. Published on 11 June 2025. Downloaded on 2/11/2026 11:18:29 AM.
This article is licensed under a Creative Commons Attribution-NonCommercial 3.0 Unported Licence.

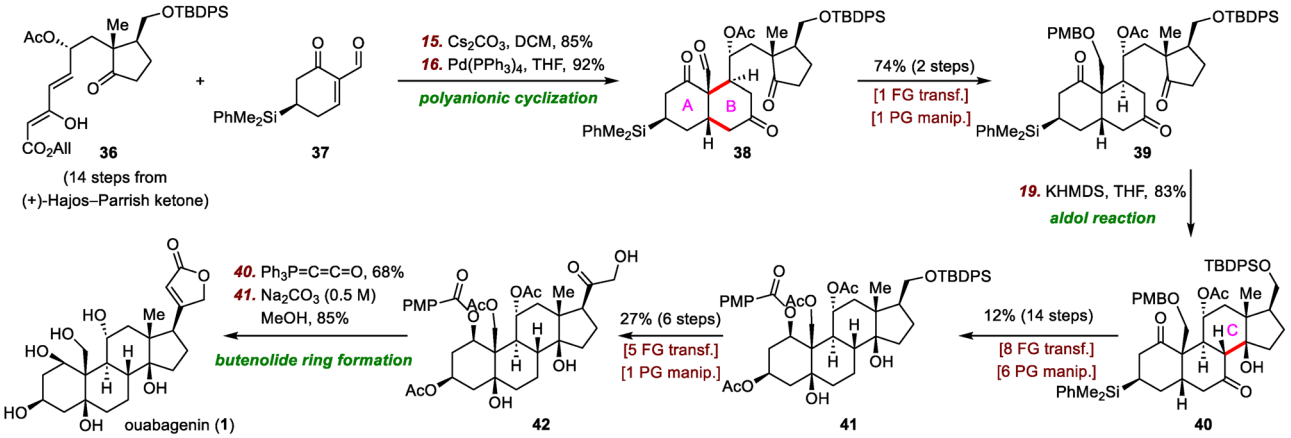

Abbreviations: TBDPS = *tert*-butyldiphenylsilyl; All = allyl; DCM = dichloromethane; PPh_3 = triphenylphosphine; THF = tetrahydrofuran; PMB = *para*-methoxybenzyl; KHMDS = potassium *bis*(trimethylsilyl)amide; PMP = *para*-methoxyphenyl.

Scheme 7 Deslongchamps's synthesis of ouabagenin (**1**).

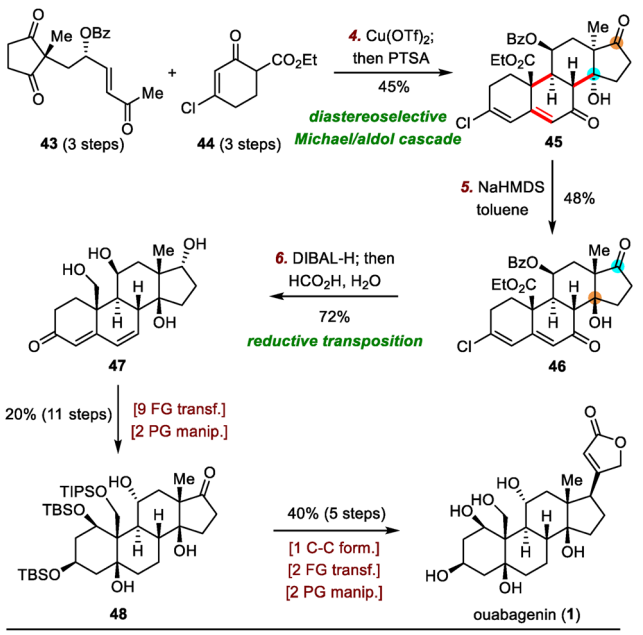

Abbreviations: Bz = benzoyl; PTSA = *p*-toluenesulfonic acid; NaHMDS = sodium *bis*(trimethylsilyl)amide; DIBAL-H = diisobutylaluminum hydride; TIPS = triisopropylsilyl.

Scheme 8 Nagorny's synthesis of ouabagenin (**1**).

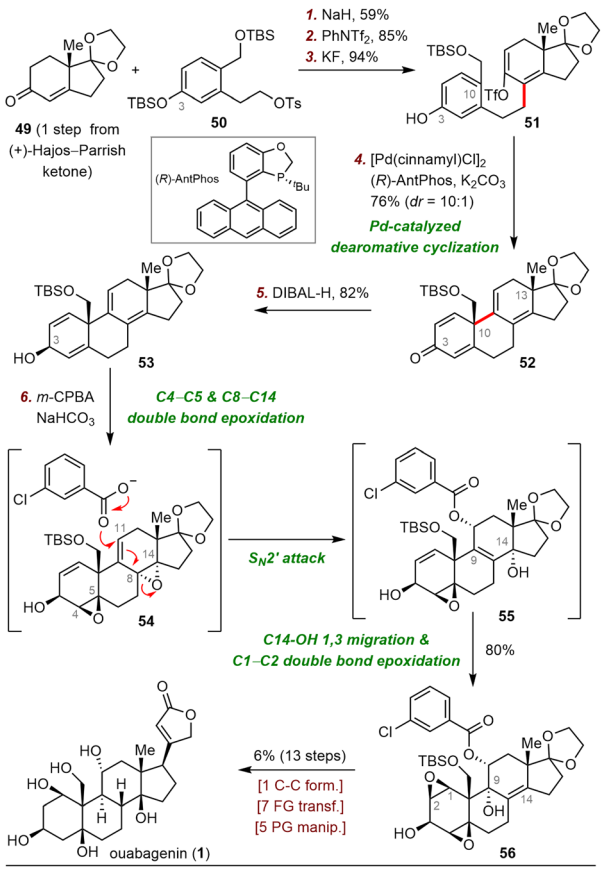

Abbreviation: *m*-CPBA = *meta*-chloroperoxybenzoic acid.

Scheme 9 Tang's synthesis of ouabagenin (**1**).

C3 *tert*-butyl(dimethyl)silyl (TBS) group to yield phenol **51**, which was the precursor for the dearomative cyclization reaction. Pleasingly, palladium-catalyzed enantioselective dearomative cyclization of **51** in the presence of (*R*)-AntPhos as a ligand smoothly gave dienone **52** in 76% yield with a 10 : 1 diastereomeric ratio (dr) at C10. In contrast, replacing (*R*)-AntPhos with (*rac*)-AntPhos led to a poor dr (1.5 : 1), indicating that the stereochemistry at C13 had little influence on the stereochemistry at C10.

With compound **52**, which possesses the desired tetracyclic framework, in hand, Tang and colleagues had reached the stage for installing multiple hydroxyl groups onto the skeleton. To this end, reduction of the C3-ketone of **52** with DIBAL-H delivered alcohol **53**, which was epoxidized with *m*-chloroperoxybenzoic acid (*m*-CPBA) to produce diepoxide **56** in 80% yield. After characterizing two key intermediates during the above-described process, Tang *et al.* proposed the following plausible pathway: (1) diastereoselective epoxidation of the C4–C5 and C8–C14 double bonds gives **54**, (2) S_N2' attack at

Open Access Article. Published on 11 June 2025. Downloaded on 2/11/2026 11:18:29 AM.
This article is licensed under a Creative Commons Attribution-NonCommercial 3.0 Unported Licence.

C11 of **54** produces allylic alcohol **55**, and (3) 1,3-migration of the allylic alcohol from C14 to C9 and subsequent C3-OH-directed epoxidation of the C1–C2 double bond generate **56**. Ouabagenin (**1**) was synthesized from **56** in thirteen steps.

2.2.4. Luo's synthesis of wortmannin. Phosphatidylinositol 3-kinase is an attractive target for cancer therapy drugs owing to the enzyme's strong correlation with cell growth, survival, and so on.[42] Among various selective inhibitors of this enzyme, wortmannin (**2**) is a standout because of its low-nanomolar *in vitro* half-maximal inhibitory concentration (IC_{50}).[43]

Wortmannin belongs to the furanosteroid subclass of steroids and was originally isolated from *Penicillium wortmannii*.[44] This natural product possesses a highly reactive [6,6,5]-furanocyclohexadienone lactone moiety and two all-carbon quaternary stereogenic centers, one at C10 and another at C13. The highly oxidized skeleton of wortmannin, coupled with its biological importance, has gained tremendous attention from the synthetic organic community, which culminated in two synthetic routes by Shibasaki[45] and one route by Luo.[46] In 1996, Shibasaki and co-workers accomplished a semisynthesis of wortmannin from hydrocortisone.[45a] In 2002, they developed a second strategy which involved the use of an intramolecular Heck reaction to construct the B ring and the synthetically challenging C10 quaternary stereogenic center.[45b] Using the second strategy, these investigators accomplished a formal enantioselective synthesis of wortmannin in 2005.[45c]

Luo's 2017 synthesis featured convergent assembly of the B ring *via* a palladium-catalyzed cascade reaction and an intramolecular Friedel–Crafts alkylation to forge the C7–C8 and C5–C10 bonds, respectively (Scheme 10).[46] The synthesis began with a coupling reaction between carboxylic acid **57** and propargyl carbonate **58** in the presence of $Pd_2(dba)_3$ (dba, dibenzylideneacetone) *via* a π-propargyl-palladium species to afford furan **59**. In contrast, direct alkylation of (+)-Hajos–Parrish ketone with a halofuran electrophile resulted in double alkylation and required a lengthy preparation of the electrophilic reagent. Furan **59** was transformed into epoxide **60** in six steps, setting the stage for the second key bond-forming reaction. Specifically, the use of hexafluoro-2-propanol as a solvent and Ph_4PBF_4 as an additive facilitated the desired Friedel–Crafts alkylation at the β-position of the furan with the epoxide to give a tetracyclic intermediate (not shown), which then underwent desilylation to afford **61** in 47% yield over two steps. Compound **61** was elaborated to wortmannin (**2**) in nine steps.

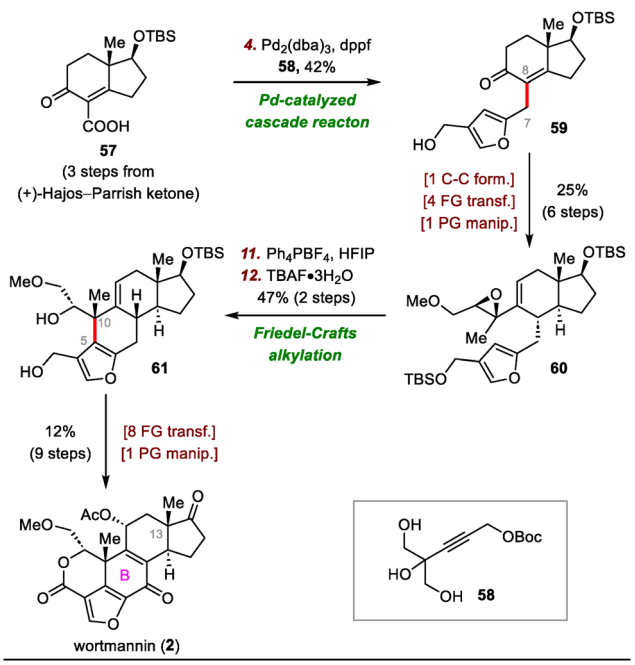

Abbreviations: dba = dibenzylideneacetone; HFIP = 1,1,1,3,3,3-hexafluoro-2-propanol; TBAF = tetra-*n*-butylammonium fluoride; Boc = *tert*-butoxycarbonyl.

Scheme 10 Luo's synthesis of wortmannin (**2**).

2.2.5. Guerrero's syntheses of viridin and viridiol. The furanosteroids viridin (**67**)[47] and viridiol (**3**)[48] are antifungal metabolites found in *Gliocladium virens* and *Trichoderma viride*, respectively. Viridiol can be viewed as a dihydro derivative of viridin, and bioconversion of viridin to viridiol has been reported.[49] In addition, the biosynthetic pathway for the furanosteroid natural product demethoxyviridin has been extensively studied.[50] Viridin and viridiol share a highly oxidized tetracyclic steroidal framework fused with a furan ring between C4 and C6, which is similar to the wortmannin framework. However, although the biological importance of wortmannin has been extensively documented, the biological profiles of vididin and viridiol have rarely been studied.[51]

To date, three impressive total syntheses of viridin and viridiol have been reported, one each by the groups of Sorensen,[52] Guerrero,[53] and Gao.[54] In 2004, Sorensen and co-workers disclosed the first asymmetric total syntheses of viridin and viridiol, which were accomplished by means of a rhodium-catalyzed cyclotrimerization to form the tetrasubstituted phenyl ring (C ring) and a thermal electrocyclic rearrangement to establish the B ring.

Guerrero's synthetic strategy was based mainly on bond disconnection at the central B ring (Scheme 11).[53] The synthesis commenced with a Liebeskind stannane-thioester coupling reaction between furan **62** and indanone **63**, furnishing diketone **64** in 83% yield. Products resulting from oxidative addition of the aryl triflate were not observed. Ketone **64** underwent a highly enantioselective palladium-catalyzed intramolecular Heck reaction to forge the B ring, giving rise to alkene **65** in 75% yield with high enantioselectivity (>99% enantiomeric excess).[55] Overall, these key C–C bond forming reactions allowed for quick construction of the pentacyclic skeleton of viridin and viridiol in only two steps from simple building blocks. Elaboration of **65** to viridiol (**3**) required seven steps. Finally, oxidation of viridiol (**3**) with catalysis by (2,2,6,6-tetramethylpiperidin-1-yl)oxyl (TEMPO) furnished viridin (**67**) in 46% yield.

2.2.6. Gao's syntheses of viridin and viridiol. In 2019, Gao and co-workers also reported asymmetric total syntheses of viridin and viridiol, which were accomplished by means of an intramolecular [3+2] cycloaddition to construct the highly oxidized A ring and a metal-hydride hydrogen atom transfer radical cyclization to form the B ring (Scheme 12).[54] Condensation of hemiacetal **68** with hydroxylamine gave an oxime intermediate

 This journal is © The Royal Society of Chemistry 2025

Open Access Article. Published on 11 June 2025. Downloaded on 2/11/2026 11:18:29 AM.
This article is licensed under a Creative Commons Attribution-NonCommercial 3.0 Unported Licence.

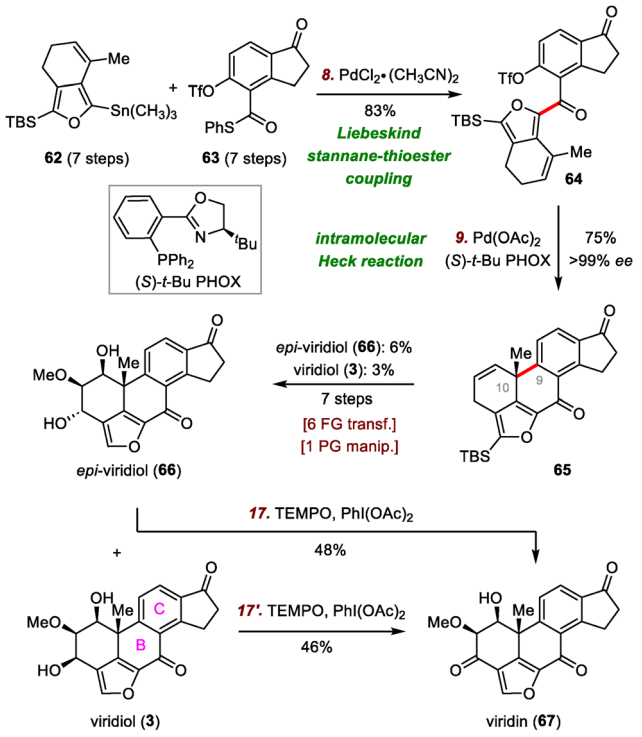

Scheme 11 Guerrero's syntheses of viridin (**67**) and viridiol (**3**).

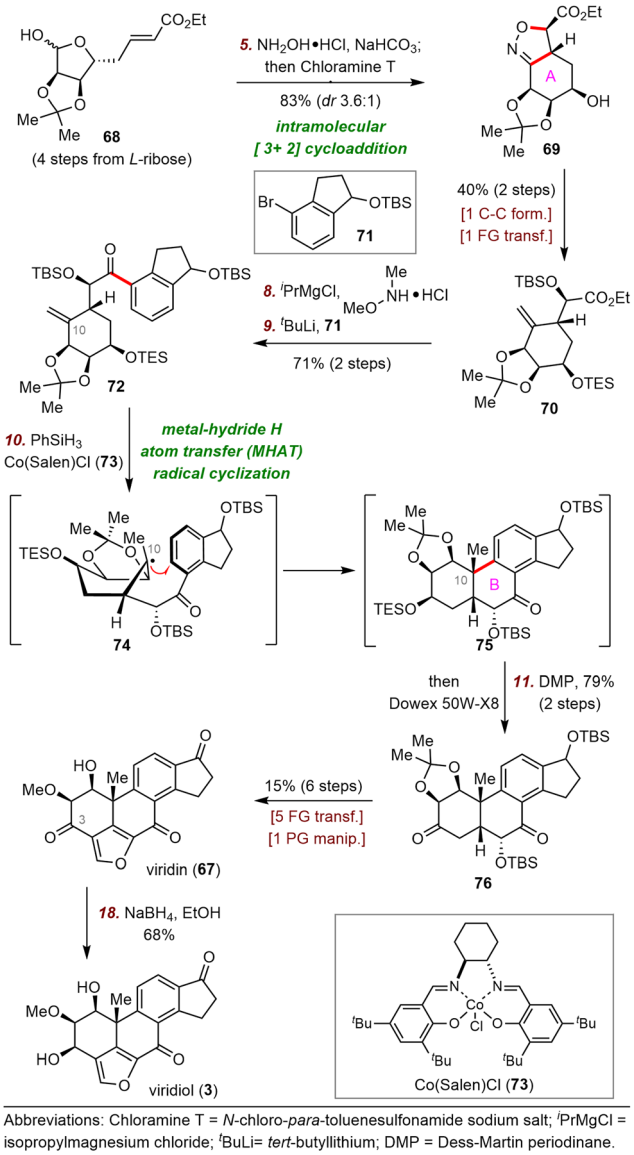

Scheme 12 Gao's syntheses of viridin (**67**) and viridiol (**3**).

(not shown). The oxime intermediate was oxidized with Chloramine T to generate a nitrile oxide, which underwent subsequent intramolecular [3+2] cycloaddition to furnish isoxazoline **69** in 83% yield with 3.6 : 1 dr. A two-step sequence transformed **69** to ester **70**. This compound was then converted to the corresponding Weinreb amide, which underwent nucleophilic addition with a lithium reagent derived from bromide **71** and *tert*-butyllithium (^{t}BuLi) to furnish ketone **72** in 71% yield over two steps.

Next, treatment of alkene **72** with Co(Salen)Cl (**73**) in the presence of phenylsilane ($PhSiH_3$) resulted in a radical cyclization reaction that furnished desired tetracyclic ketone **75**.[56] The cyclization may have proceeded *via* radical intermediate **74**, which led to desired stereochemistry at C10 *via* conformational control. Ketone **75** was then transformed to viridin (**67**) in seven steps, and selective reduction of the C3-ketone of viridin with sodium borohydride ($NaBH_4$) uneventfully provided viridiol (**3**) in 68% yield.

2.2.7. Ma's syntheses of dankasterones A and B and periconiastone A. The 13(14 → 8)*abeo*-steroids dankasterones A ($\Delta^{4,5}$-**8**) and B (**8**) and periconiastone A (**9**) belong to a novel class of ergostane-like steroids. Dankasterones A[57] and B[58] were isolated by Numata and co-workers in 1999 and 2007, respectively; and periconiastone A was isolated more recently (2019), by the Zhang group.[59] In contrast to dankasterones A and B, which have a 6/6/5/6 tetracyclic framework, periconiastone A has an unprecedented 6/6/6/6/5 pentacyclic skeleton that is thought to be biogenetically derived from dankasterone B *via* an intramolecular aldol reaction between C4 and C14. In terms of biological activities, both dankasterones A and B inhibit the growth of murine P388 cancer cells, and periconiastone A exhibits activities against the Gram-positive bacteria *Staphylococcus aureus* and *Enterococcus faecalis*, with minimum inhibitory concentrations of 4 and 32 μg mL^{-1}, respectively.

In 2022, Heretsch reported the first syntheses of dankasterones A and B and periconiastone A, which were accomplished by means of a radical framework reconstruction strategy.[60] Shortly after Heretsch's semisynthesis, Ma and co-workers reported their total syntheses of these *abeo*-steroids, wherein radical cyclization mediated by metal-hydride hydrogen atom transfer was employed to construct the *cis*-decalin framework (Scheme 13).[61]

Ma's syntheses began with the union of chiral fragments **77** and **78** *via* nucleophilic addition and Dess–Martin periodinane oxidation of the resulting secondary alcohol, generating enone

Open Access Article. Published on 11 June 2025. Downloaded on 2/11/2026 11:18:29 AM.
This article is licensed under a Creative Commons Attribution-NonCommercial 3.0 Unported Licence.

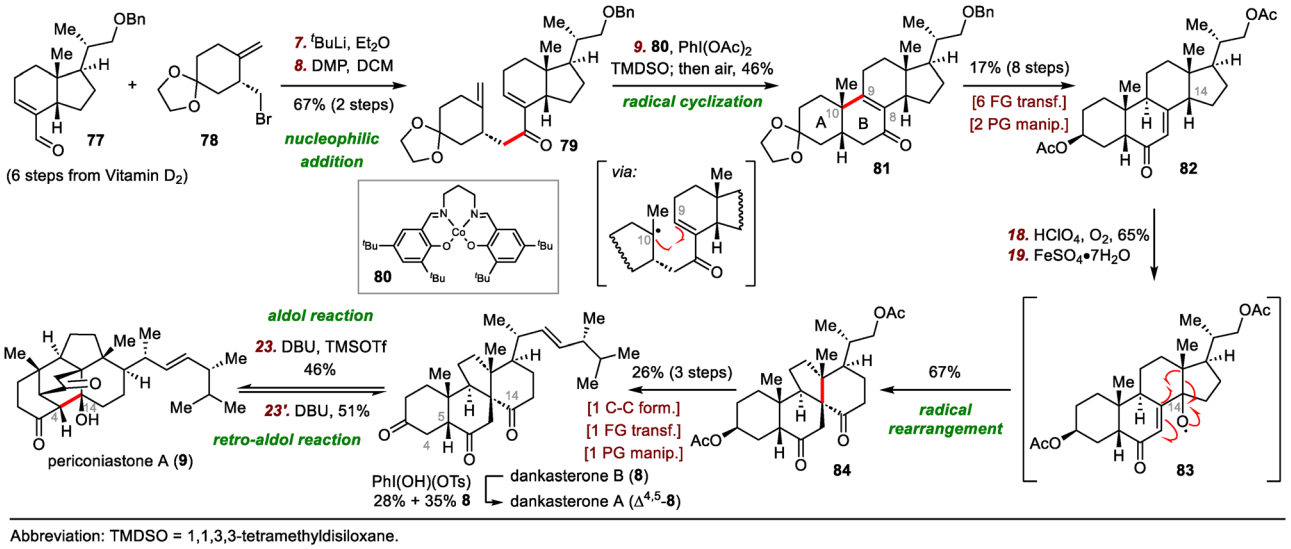

Scheme 13 Ma's syntheses of dankasterones A ($\Delta^{4,5}$-**8**) and B (**8**) and periconiastone A (**9**).

79 in 67% yield over two steps. After extensive optimization of various reaction parameters, tetracyclic compound **81**, which has the desired *cis*-fused A/B ring system, was obtained in 46% yield by cycloisomerization of **79**. A cobalt catalyst was found to be superior to iron and manganese catalysts:[62] $Fe(dpm)_3$ (dpm, 2,2,6,6-tetramethylheptane-3,5-dionate) delivered the desired Giese-type cyclization product (not shown) but in only 33% yield with reduction of the C8–C9 bond, and all attempts with manganese catalysts failed to give any useful products.

Compound **81** was transformed to enone **82** in eight steps, setting the stage for the pivotal radical rearrangement to build the 13(14 → 8)*abeo*-steroid skeleton. Specifically, treatment of enone **82** with O_2 in the presence of perchloric acid ($HClO_4$) led to the formation of a C14 hydroperoxide intermediate, which underwent radical rearrangement to afford desired product **84** in 67% yield, possibly *via* radical intermediate **83**. Finally, spirocycle **84** was converted to dankasterone B (**8**) in three steps. Selective dehydrogenation of **8** at C4–C5 delivered dankasterone A ($\Delta^{4,5}$-**8**). Furthermore, biomimetic interconversion of **8** and periconiastone A (**9**) through intramolecular aldol and retro-aldol reactions was achieved with 1,8-diazabicyclo[5.4.0]undec-7-ene (DBU).

2.2.8. Our group's syntheses of clionastatins A and B. Clionastatins A (**91**) and B (**4**) are tri- and tetrachlorinated androstane derivatives, respectively, that were isolated in 2004 from the burrowing sponge *Cliona nigricans* by Fattorusso and coworkers.[63] The highly unsaturated tetracyclic frameworks of these natural products, as well as their potent cytotoxicity against several tumor cell lines (half-maximal inhibitory concentrations range from 0.8 to 2.0 μg mL^{-1}), have attracted considerable interest from the synthetic community. In 2021, our group reported the first asymmetric total syntheses of clionastatins A and B, which were accomplished by means of an acyl radical conjugate addition reaction followed by an intramolecular Heck cyclization to assemble the key tetracyclic skeleton (Scheme 14).[64] It is worth mentioning that this work resulted in a revision of the stereochemistry at C14 to the β-H configuration rather than the initially proposed α-H configuration. In 2022, Zhang and coworkers disclosed semisyntheses of clionastatins A and B through a unique two-stage chlorination/oxidation strategy.[65]

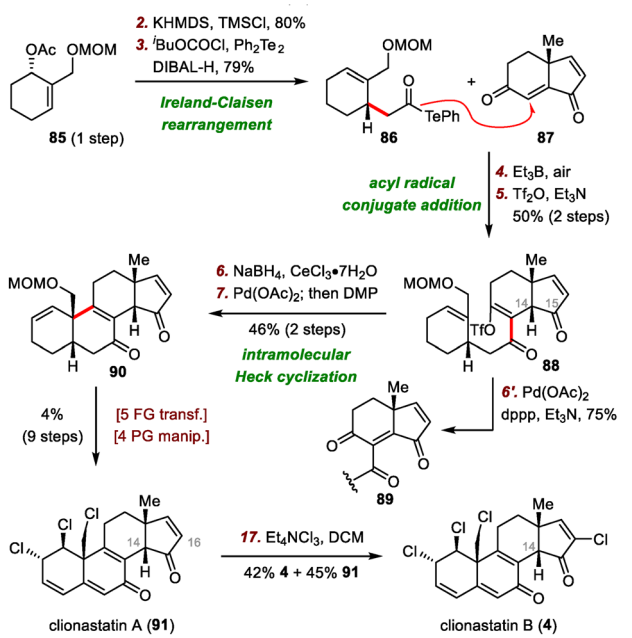

Scheme 14 Our group's syntheses of clionastatins A (**91**) and B (**4**).

Our group's syntheses started with the preparation of donor **86** for the acyl radical conjugate addition reaction. To this end, an Ireland–Claisen rearrangement of chiral allylic acetate **85** with KHMDS and trimethylsilyl chloride afforded an 80% yield of a carboxylic acid intermediate, which was converted to acyl telluride **86** in 79% yield. Upon treatment with triethyl borane (Et_3B) and air, **86** smoothly underwent an acyl radical conjugate addition reaction with enone **87**,[66] affording a triketone

 This journal is © The Royal Society of Chemistry 2025

Open Access Article. Published on 11 June 2025. Downloaded on 2/11/2026 11:18:29 AM.
This article is licensed under a Creative Commons Attribution-NonCommercial 3.0 Unported Licence.

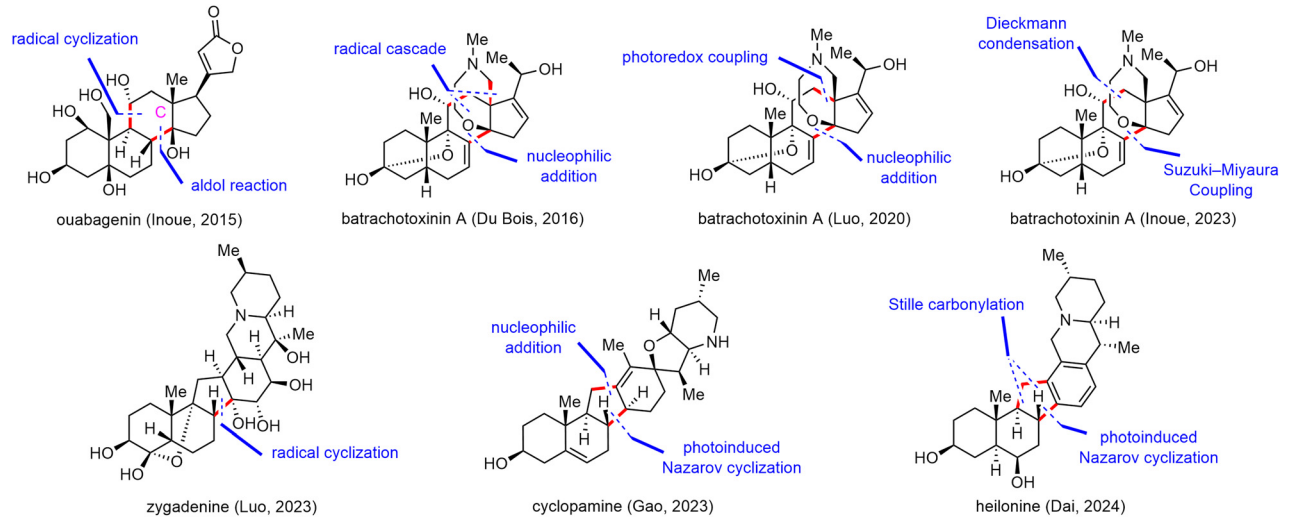

Scheme 15 Retrosynthetic disconnections at the C ring.

intermediate that was transformed to enol triflate **88** in 50% yield over two steps. Unfortunately, direct Heck cyclization[67] of **88** failed to provide any cyclized product; triketone **89** was the only product (75% yield). Formation of **89** could be attributed to the extremely high acidity of C14–H, which is located at the α-position relative to the ketone at C15. This problem was avoided by subjecting **88** to a Luche reduction to give a mixture of diols, which underwent the desired Heck cyclization reaction to furnish enone **90** (46% yield over two steps) after *in situ* oxidation of the cyclized diols with Dess–Martin periodinane (DMP).

With tetracyclic enone **90** in hand, we adjusted the oxidation states and installed the alkyl chloride and vinyl chloride functional groups. Specifically, clionastatin A (**91**) was obtained from **90** in nine steps. Selective chlorination of **91** at C16 furnished clionastatin B (**4**).

2.3. Convergent assembly of the C ring

Like disconnection at the B ring (Scheme 6), disconnection at the C ring leads to two fragments of comparable structural complexity (the A/B ring system and the D ring), and this disconnection has also been widely recognized as an efficient strategy for steroid synthesis (Scheme 15). In this subsection, representative recent synthetic work on building the C ring and associated stereogenic centers *via* various bond-forming reactions will be highlighted.

2.3.1. Inoue's synthesis of ouabagenin. In contrast to the three aforementioned strategies for the synthesis of ouabagenin, which featured a key bond disconnection at the B ring, the strategy reported by Inoue and co-workers in 2015 involved an intramolecular radical cyclization and an aldol reaction for convergent construction of the C ring (Scheme 16).[34] These investigators also used this strategy in a synthesis of 19-hydroxysarmentogenin.[68]

The Inoue group's synthesis of ouabagenin began with the joining of fragments **92** and **93** *via* nucleophilic substitution to furnish acetal **94**. Upon treatment of **94** with Et_3B and tributyltin hydride (n-Bu_3SnH) in the presence of O_2, a secondary

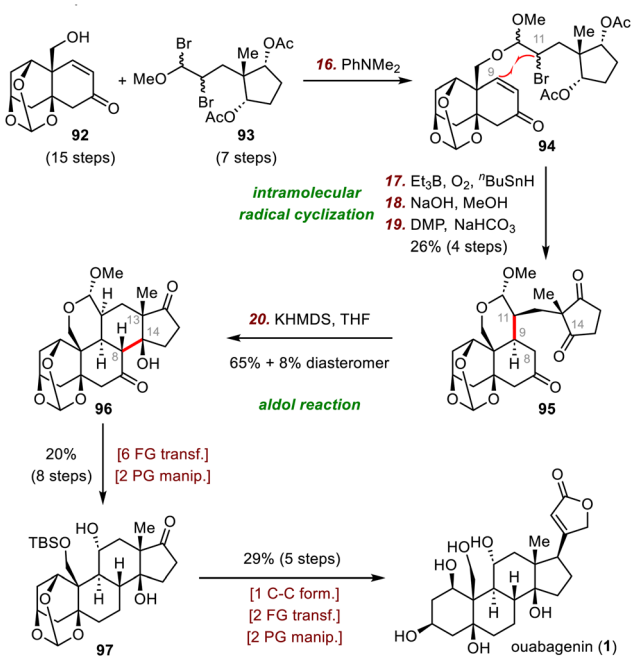

Scheme 16 Inoue's synthesis of ouabagenin (**1**).

radical generated from the bromide engaged in the desired 6-*exo* radical cyclization to form the key C9–C11 bond. Subsequent hydrolysis of the acetates and DMP oxidation of the resulting alcohols gave triketone **95** in 26% yield over four steps. Next, an intramolecular aldol reaction between C8 and C14 of **95** in the presence of KHMDS as the base afforded **96** (65% yield), which has the desired tetracyclic skeleton, along with an 8% yield of the diastereomer with the opposite configurations at C13 and C14. Further elaboration (eight steps) afforded diol **97**, which was transformed to ouabagenin (**1**) in five steps.

2.3.2. Du Bois's syntheses of batrachotoxinin A and batrachotoxin. The highly oxidized steroid natural product

Open Access Article. Published on 11 June 2025. Downloaded on 2/11/2026 11:18:29 AM.
This article is licensed under a Creative Commons Attribution-NonCommercial 3.0 Unported Licence.

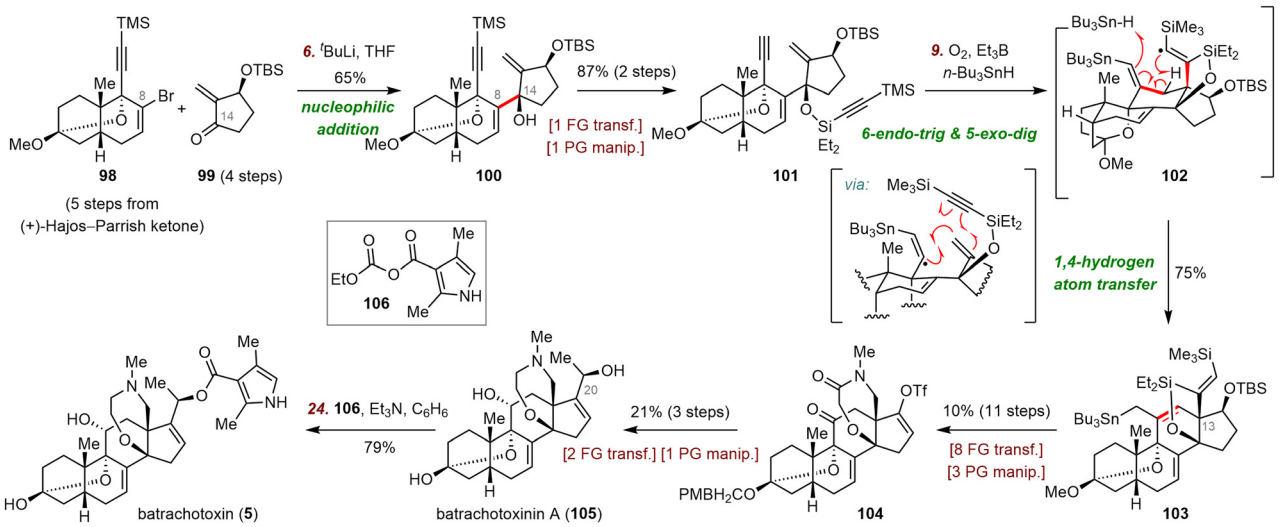

Scheme 17 Du Bois's syntheses of batrachotoxinin A (**105**) and batrachotoxin (**5**).

batrachotoxin (**5**) was isolated from the skin of an endangered *Phyllobates* poison-dart frog.[69] Batrachotoxin is a potent voltage-gated sodium channel modulator.[70] In contrast, batrachotoxinin A (**105**), which lacks the pyrrole ester of **5**, displays weaker biological activity.[71] However, batrachotoxinin A can be converted to batrachotoxin and analogues for structure–activity relationship studies.

In 1972, Imhof and co-workers reported a semisynthesis of batrachotoxinin A,[72] and the first total synthesis of this molecule was achieved by the Kishi group in 1998.[73] Subsequent total syntheses of batrachotoxin and batrachotoxinin A were reported by the groups of Du Bois,[74] Luo,[75] and Inoue.[76]

Du Bois's syntheses of batrachotoxinin A and batrachotoxin commenced with a nucleophilic addition reaction between enone **99** and the vinyl lithium species (generated by reaction of vinyl bromide **98** with ^{t}BuLi) to furnish enyne **100** (65% yield), which has the key C8–C14 bond (Scheme 17). Enyne **100** was transformed to **101** in two steps, setting the stage for a radical cascade cyclization to install the C ring and the all-carbon quaternary stereocenter at C13. To this end, treatment of **101** with Et_3B and *n*-Bu_3SnH in the presence of O_2 produced a vinyl radical intermediate (not shown), which underwent successive 6-*endo*-trig and 5-*exo*-dig radical cyclizations followed by 1,4-hydrogen atom transfer of vinyl radical intermediate **102** to afford **103** in 75% yield. This unprecedented enyne radical cyclization afforded the tetracyclic skeleton of batrachotoxin in only four steps from fragments **98** and **99**.

Subsequently, a series of redox manipulations furnished batrachotoxin and batrachotoxinin A. Specifically, elaboration of **103** led to vinyl triflate **104**, which was converted to batrachotoxinin A (**105**) in three steps. Esterification of batrachotoxinin A with mixed anhydride **106** furnished batrachotoxin (**5**) in 79% yield.

2.3.3. Luo's synthesis of batrachotoxinin A. In 2020, Luo and co-workers reported their asymmetric total synthesis of batrachotoxinin A (Scheme 18).[75] The synthesis featured a

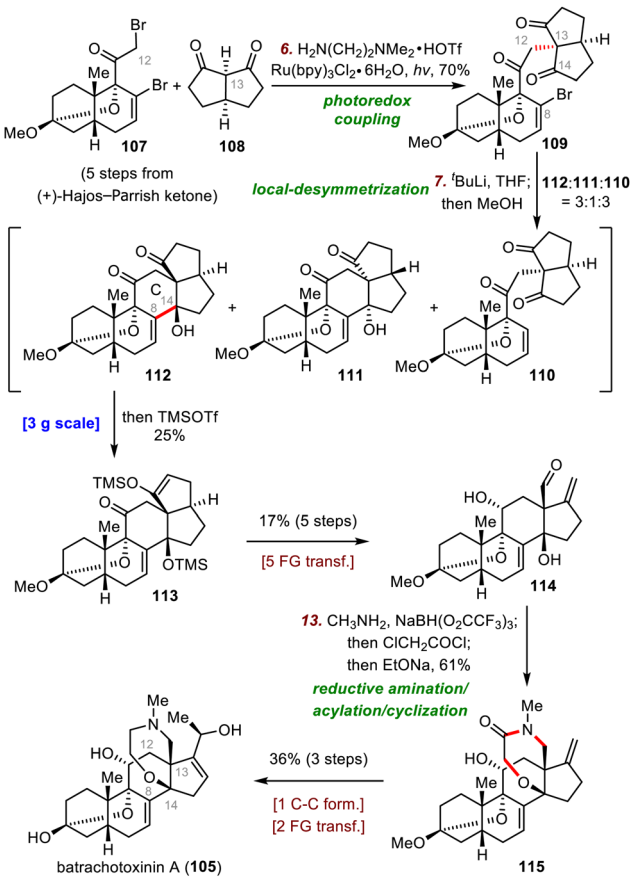

Scheme 18 Luo's synthesis of batrachotoxinin A (**105**).

photoredox coupling reaction and a local-desymmetrization nucleophilic addition to forge the C12–C13 and C8–C14 bonds, respectively, both of which are located in the C ring.

A powerful photoredox alkylation reaction that was first developed by the MacMillan group for asymmetric photoalkylation of aldehydes[77] and later improved by the Luo group for asymmetric

 This journal is © The Royal Society of Chemistry 2025

Open Access Article. Published on 11 June 2025. Downloaded on 2/11/2026 11:18:29 AM. This article is licensed under a Creative Commons Attribution-NonCommercial 3.0 Unported Licence.

α-photoalkylation of β-ketocarbonyls[78] was found to be exceptionally useful for photoredox coupling of bromide **107** and diketone **108** to furnish vinyl bromide **109** in 70% yield. In contrast, all attempts to construct the C12–C13 bond *via* traditional S_N2 reactions failed. Subsequently, closure of the C ring was pursued by means of a local-desymmetrization nucleophilic addition reaction between C8 and C14. Specifically, treatment of **109** with ^{t}BuLi at −98 °C gave a 3 : 1 : 3 mixture of desired alcohol **112**, diastereomer **111**, and debromination product **110**, and *in situ* silylation of desired product **112** gave silyl enol ether **113** in 25% yield. Although the yield of the desired cyclized product was modest, the reaction could be easily performed on a 3 g scale, providing enough material for the following transformations. **113** was converted to aldehyde **114** in five steps, and then a one-pot reductive amination/acylation/cyclization of **114** was employed to build the homomorpholinamide ring: **115** was obtained in 61% yield, thereby forming the required ring system. Finally, **115** was converted to batrachotoxinin A (**105**) in three steps.

2.3.4. Inoue's syntheses of batrachotoxinin A and batrachotoxin. Inoue's total syntheses of batrachotoxinin A and batrachotoxin represent additional examples in which bond disconnection in the C ring of a highly oxidized steroid natural product greatly simplified the synthesis, because it led to two fragments with similar complexity (**116** and **117**, Scheme 19).[76]

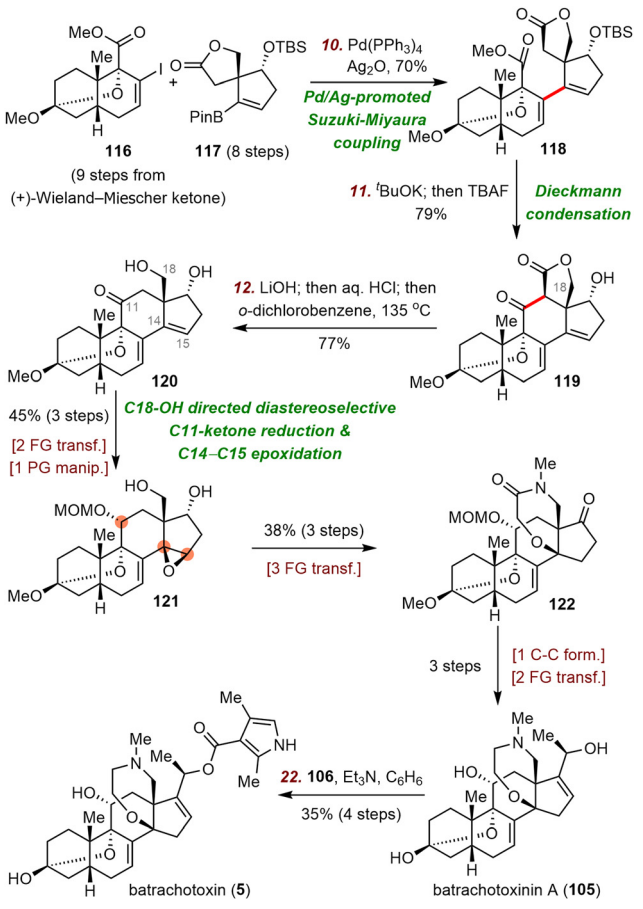

Scheme 19 Inoue's syntheses of batrachotoxinin A (**105**) and batrachotoxin (**5**).

First, Inoue *et al.* used a Suzuki–Miyaura coupling reaction[79] to connect two chiral fragments, vinyl iodide **116** and pinacol boronate **117**, delivering ester **118** in 70% yield. Subsequent potassium *tert*-butoxide (^{t}BuOK)-promoted intramolecular Dieckmann condensation and one-pot desilylation led to lactone **119** in 79% yield. Saponification and subsequent decarboxylation at high temperature released the C18-alcohol, giving rise to diol **120**. This compound underwent C18-alcohol-directed diastereoselective C11-ketone reduction and C14–C15 epoxidation to deliver **121** in three steps. Alcohol **121** was transformed to batrachotoxinin A (**105**) in six steps, and esterification of batrachotoxinin A gave batrachotoxin (**5**).

2.3.5. Luo's syntheses of *Veratrum* alkaloids. The highly oxidized C-*nor*-D-*homo* steroidal alkaloids zygadenine (**12**),[80] germine (**131**),[81] and protoverine (**132**)[82] belong to the cevanine family of compounds, which have been isolated from flowering plants of the *Veratrum* genus.[83] Several members of this family have been found to exhibit a diverse array of biological activities.[83b] In 2023, Luo and co-workers reported the first total synthesis of zygadenine (Scheme 20), featuring an intramolecular Diels–Alder reaction followed by a radical cyclization to construct the hexacyclic carbon skeleton.[84] In 2024, these investigators accomplished divergent syntheses of germine, protoverine, and the alkamine of veramadine A by means of a late-stage neighboring-group participation strategy to stereoselectively install several synthetically challenging oxidation states.[85]

First, chiral furan **123**, accessed from (+)-Hajos–Parrish ketone in six steps, was oxidized by $^1O_2$, and pyridine-catalyzed isomerization of the resulting electron-deficient *cis* olefin and Pinnick oxidation of the aldehyde intermediate furnished carboxylic acid **124** in 87% yield over two steps.[84] Conversion of **124** into the corresponding anhydride was followed by amidation with free amine **126** (prepared from **125** in six steps) to afford amide **127**. The amide was heated to reflux in THF to promote the intramolecular Diels–Alder reaction, which furnished bromide **128** in 92% yield. Moving forward, the crucial C8–C14 bond was established by means of an intramolecular radical cyclization, affording cyanide **129** in 89% yield after *in situ* reduction of the C11 ketone. In this way, the hexacyclic carbon framework was constructed in only ten steps. With sufficient quantities of **129** in hand, Luo *et al.* divergently synthesized *Veratrum* alkaloids zygadenine (**12**), the alkamine of veramadine A (**130**), germine (**131**), and protoverine (**132**) through judicious application of a series of redox manipulations.[85]

2.3.6. Gao's syntheses of veratramine and cyclopamine. The C-*nor*-D-*homo* steroidal alkaloids veratramine (**13**)[86] and cyclopamine (**14**)[87] belong to the veratramine and jervanine subgroups of *Veratrum* alkaloids, respectively. Veratramine exhibits activity against androgen-independent prostate cancer cells,[88] and cyclopamine is a potent inhibitor of the hedgehog signaling pathway.[89] The first synthesis of veratramine was reported in 1967 by the Johnson group, who utilized a semisynthetic strategy.[90] In 2009, Giannis and co-workers reported a semisynthesis of cyclopamine featuring a bioinspired skeletal reorganization strategy.[91] A convergent total synthesis of cyclopamine was disclosed by Baran and co-workers in 2023.[92] In 2023 and 2024, the groups of Gao[93] and Qin[94] accomplished concise syntheses of veratramine and

Open Access Article. Published on 11 June 2025. Downloaded on 2/11/2026 11:18:29 AM.
This article is licensed under a Creative Commons Attribution-NonCommercial 3.0 Unported Licence.

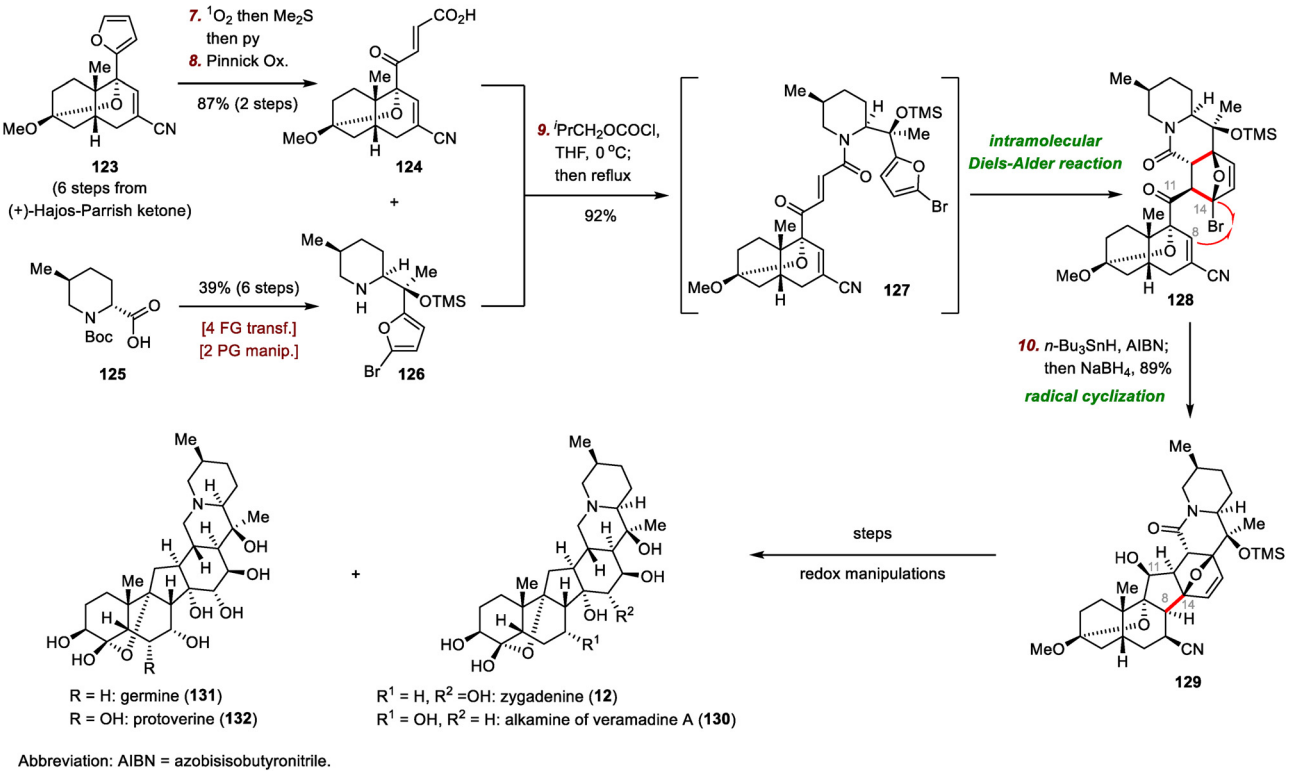

Scheme 20 Luo's syntheses of *Veratrum* alkaloids.

cyclopamine, respectively. Very recently, Trauner and co-workers disclosed a convergent synthesis of veratramine and 20-iso-veratramine *via* a key aromative Diels–Alder reaction.[95]

The synthesis of cyclopamine by Gao and co-workers began with preparation of compound **135**, the precursor for a photo-induced excited-state Nazarov cyclization (Scheme 21).[93] To this end, nucleophilic addition of an aryl lithium species (generated by a lithium/bromide exchange reaction between **133** and ^{t}BuLi) to aldehyde **134** gave a secondary alcohol, which was oxidized to deliver enone **135** in 52% yield over two steps. The subsequent Nazarov cyclization proceeded smoothly upon irradiation of **135** with UV light (366 nm),[96] generating tetracyclic intermediate **137** in 67% yield, possibly *via* disrotatory electrocyclization of **136**. Intermediate **137** was transformed into veratramine (**13**) in two steps. Veratramine served as the starting material for a relay synthesis of cyclopamine (**14**). Specifically, a four-step sequence converted **13** to epoxide **138**, which underwent acid-induced cyclization to afford tertiary alcohol **139**. Finally, **139** was elaborated to cyclopamine (**14**) *via* dehydration and deprotection in two steps.

2.3.7. Dai's synthesis of heilonine. The C-*nor*-D-*homo* steroidal alkaloid heilonine (**15**) is another member of the cevanine subgroup of *Veratrum* alkaloids.[97] It has the same skeleton as zygadenine (**12**) but is less oxidized. The first total synthesis of heilonine was reported in 2021 by the Rawal group, who employed an enantioselective Diels–Alder reaction to construct the chiral B ring and a rhodium-catalyzed [2+2+2] cycloisomerization to build the tetrasubstituted phenyl ring.[98] In 2024, Dai and co-workers disclosed another route to heilonine, featuring regioselective C–H functionalizations and a Stille carbonylative cross-coupling followed by a photoinduced Nazarov cyclization to build the hexacyclic skeleton.[99]

The synthesis began with a *tert*-butyloxycarbonyl (Boc)–directed C–H lithiation of **141** followed by transmetalation with $ZnCl_2$ to generate an organozinc reagent (Scheme 22), which was coupled with vinyl iodide **140** *via* a Negishi cross-coupling to furnish chiral piperidine **142** in two steps after removal of the Boc group. Hydrogenation of the *exo*-methylene group of **142** using Crabtree's catalyst was followed by free amine–directed carbonylative C–H lactamization to generate lactam **143**. The newly formed lactam moiety then served as a directing group for a rhodium-catalyzed C–H iodination of **143** to install an *ortho* iodide atom, giving iodide **144** in 85% yield. Reduction of the lactam moiety of **144** produced piperidine **145** in 95% yield, which underwent palladium-catalyzed Stille carbonylative coupling with A/B ring system **146** (prepared in seven steps from Wieland–Miescher ketone) to deliver ketone **147** in 73% yield, setting the stage for the Nazarov cyclization to build the hexacyclic framework. Of note, reduction of the carbonyl group of the lactam to the methylene group before cross-coupling was essential to get a high yield, probably because of the unfavorable steric effects of the carbonyl group.

After extensive optimization of reaction conditions for the Nazarov cyclization, irradiation of **147** with UV light (370 nm) in the presence of AcOH was found to lead to a mixture of diastereomers that could be epimerized at C9 *in situ* with KOH to produce a 1.7 : 1 mixture of desired cyclized product **149** and undesired product **148** in a total yield of 69%. Notably,

 This journal is © The Royal Society of Chemistry 2025

Open Access Article. Published on 11 June 2025. Downloaded on 2/11/2026 11:18:29 AM.
This article is licensed under a Creative Commons Attribution-NonCommercial 3.0 Unported Licence.

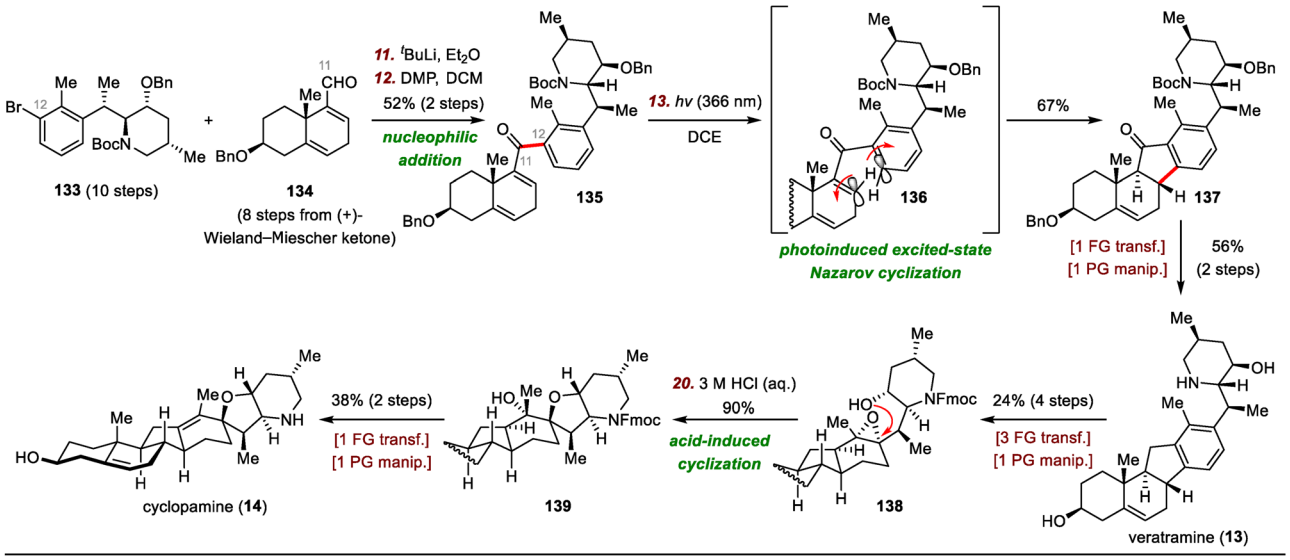

Abbreviations: DCE = 1,2-dichloroethane; Fmoc = 9-fluorenylmethoxycarbonyl.

Scheme 21 Gao's syntheses of veratramine (**13**) and cyclopamine (**14**).

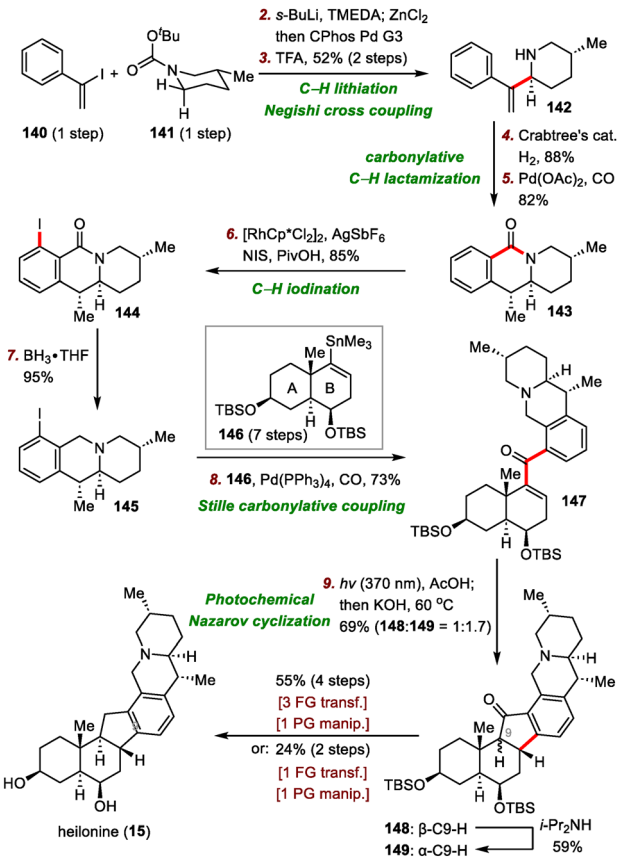

Abbreviations: TMEDA = tetramethylethylenediamine; TFA = trifluoroacetic acid; NIS = *N*-iodosuccinimide; PivOH = pivalic acid.

Scheme 22 Dai's synthesis of heilonine (**15**).

148 could be isolated and resubjected to the epimerization conditions to furnish **149** in 59% yield. Finally, **149** was converted to heilonine (**15**) in either two or four steps.

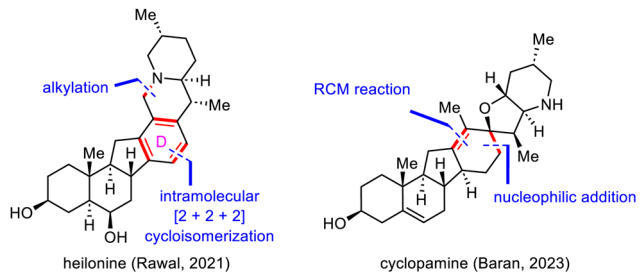

Scheme 23 Retrosynthetic disconnection at the D ring.

2.4. Convergent assembly of the D ring

Retrosynthetic bond disconnection at the D ring has not been explored as thoroughly as disconnection at the B and C rings (Scheme 23). This subsection will cover Rawal's synthesis of heilonine (**15**) by means of an intramolecular [2+2+2] cycloisomerization to install the central tetrasubstituted benzene moiety[98] and Baran's synthesis of cyclopamine (**14**) *via* a nucleophilic addition and late-stage ring-closing metathesis (RCM) reaction to build the central cyclohexene motif.[92]

2.4.1. Rawal's synthesis of heilonine. Rawal and co-workers envisioned that the synthesis of heilonine could be greatly simplified by strategic bond disconnection of the central tetrasubstituted benzene ring (D ring) *via* an alkyne cycloisomerization (Scheme 24), which would forge the C and E rings concomitantly.[98] These investigators began by using Hayashi ligand **152** to catalyze an enantioselective Diels–Alder reaction between diene **150** and dienophile **151** in the presence of trifluoroacetic acid to afford aldehyde **153** in 67% yield with 90% enantiomeric excess.[100] Aldehyde **153** was converted in six steps to alkyne **154**, from which propargyl bromide **155** was synthesized in another six steps. Propargyl bromide **155** was coupled with piperidinone **156** in the presence of NaH in dimethylformamide, providing a 93%

Open Access Article. Published on 11 June 2025. Downloaded on 2/11/2026 11:18:29 AM.
This article is licensed under a Creative Commons Attribution-NonCommercial 3.0 Unported Licence.

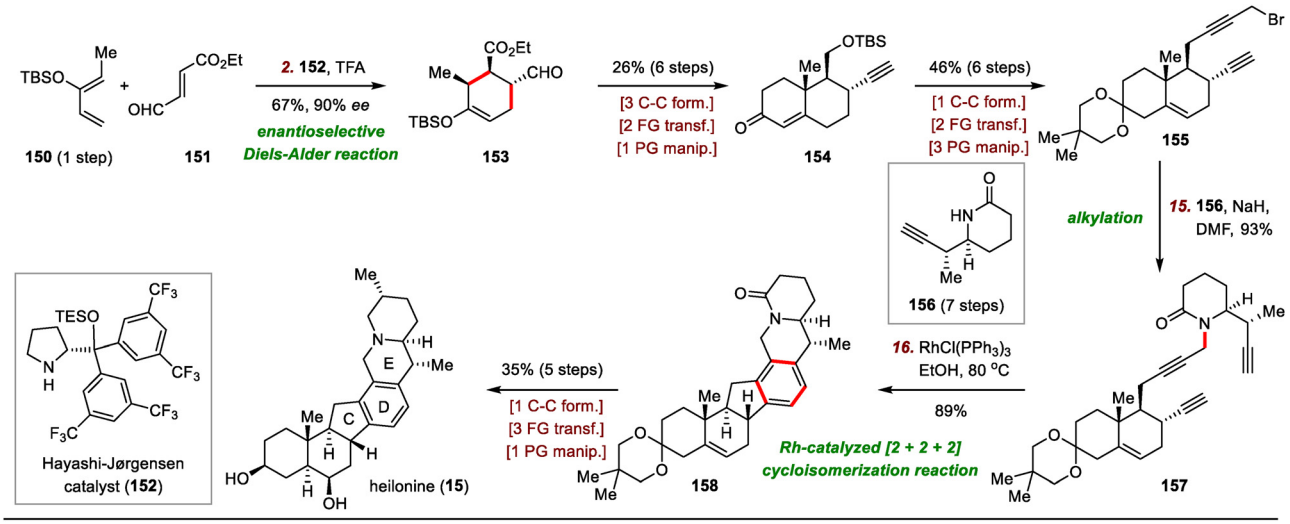

Scheme 24 Rawal's synthesis of heilonine (**15**).

yield of triyne **157**, the precursor for the key alkyne cycloisomerization. Experimentation revealed that Wilkinson's catalyst, $RhCl(PPh_3)_3$, in refluxing EtOH was optimal for promoting the alkyne cycloisomerization,[101] leading to the formation of **158**, which has the desired hexacyclic framework of heilonine. It is worth mentioning that the rhodium-catalyzed [2+2+2] cycloisomerization reaction generated the C, D, and E rings concomitantly. Compound **158** was elaborated to heilonine (**15**) in five steps.

2.4.2. Baran's synthesis of cyclopamine. The Baran group's convergent route to cyclopamine (**14**) was enabled largely by retrosynthetic bond disconnections at the D ring *via* a nucleophilic addition and a late-stage RCM reaction (Scheme 25).[92] Specifically, $LaCl_3{\cdot}2LiCl$-promoted addition of an organolithium reagent (derived from iodide **159** and ^{t}BuLi) to enone **160** smoothly furnished tertiary alcohol **161** as a single diastereomer in 71% yield. A two-step sequence involving Boc protection and desilylation of **161** delivered allylic ester **162**, which was subjected to Tsuji–Trost cyclization to form the tetrahydrofuran (E) ring with the desired stereoretention at C17, producing ether **163** in 73% yield.[102] Finally, a late-stage RCM reaction of alkene **163** to close the D ring and subsequent global deprotection using lithium 4,4′-di-*tert*-butylbiphenylide (LiDBB) delivered cyclopamine (**14**) in two steps.

3. Synthesis of SNPs *via* semisynthetic strategies

Because convergent synthesis of SNPs offers flexibility in bond disconnection and easy preinstallation of various functional groups on the coupling fragments, convergent strategies have been widely pursued, as exemplified above. However, semisynthetic strategies, which generally utilize inexpensive commercially available steroids as starting materials, have their own advantages: (1) allowing for concise syntheses by making full use of the existing 6/6/6/5 tetracyclic ring system and the stereogenic centers of the starting steroids, (2) facilitating the discovery of novel synthetic transformations of the rigid

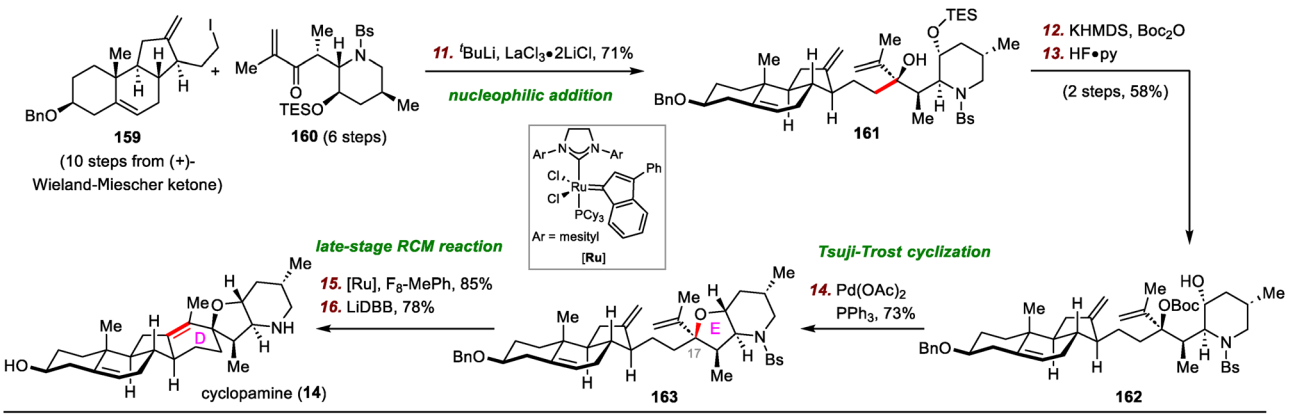

Scheme 25 Baran's synthesis of cyclopamine (**14**).

 This journal is © The Royal Society of Chemistry 2025

Open Access Article. Published on 11 June 2025. Downloaded on 2/11/2026 11:18:29 AM.
This article is licensed under a Creative Commons Attribution-NonCommercial 3.0 Unported Licence.

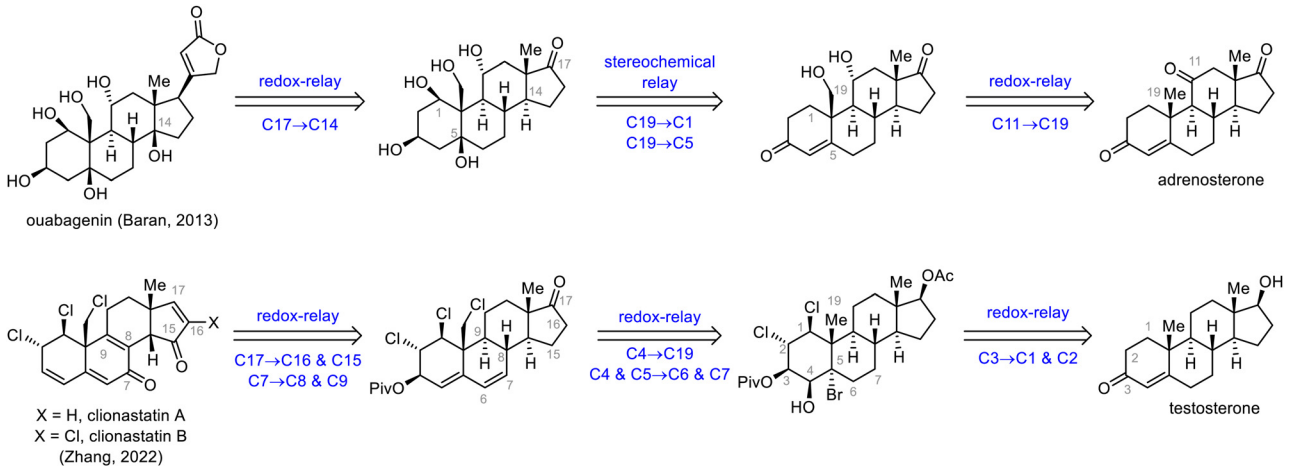

Scheme 26 Redox-relay strategies for the synthesis of highly oxidized SNPs.

framework of steroids, and (3) providing experimental evidence for proposed pathways for SNP biosynthesis. This section focuses mainly on efficient syntheses of SNPs by semisynthetic strategies. In general, these strategies pose two key challenges: (1) site-selective oxidation of the C(sp^3)–H bonds of the steroid skeletons to install the desired functional groups at specific positions and (2) skeletal reorganization of the tetracyclic skeletons of classical steroids to access the core frameworks of rearranged steroids. Accordingly, this section is divided into two subsections, one covering the redox-relay strategy and one covering the skeletal reorganization strategy.

3.1. Redox-relay strategy

Redox and stereochemical relays (Scheme 26), defined by Baran and co-workers as the transfer of redox and stereochemical information from one site to another within a molecular framework, are powerful tools for the semisynthesis of highly oxidized SNPs.[32] This strategy relies mainly on the directing effects of existing hydroxyl groups and on conformational control to achieve the desired regio- and stereoselectivities. In this subsection, the syntheses of ouabagenin by Baran *et al.*[32] and clionastatins A and B by Zhang *et al.*[65] are used to demonstrate how the oxidation states of steroids can be efficiently installed by means of a redox-relay strategy.

3.1.1. Baran's synthesis of ouabagenin. Integrating redox and stereochemical relays was key to the Baran group's scalable synthesis of ouabagenin (**1**) in 2013 (Scheme 27).[32] The synthesis started with introduction of the C19 hydroxyl group *via* a redox relay from the C11 ketone. Specifically, selective diketalization of adrenosterone (**164**) and a subsequent Norrish type II photochemical reaction of the C11 ketone generated cyclobutanol **165** in two steps, realizing functionalization of the C19 methyl group. A subsequent regioselective photolytic oxidative C–C fragmentation of **165** with *N*-iodosuccinimide as the oxidant smoothly led to C19 iodide, which was hydrolyzed with silver acetate (AgOAc) to furnish alcohol **166** in two steps. Next, stereochemical relays from the C19 hydroxyl group to C1 and C5 were accomplished *via* a three-step sequence involving C4–

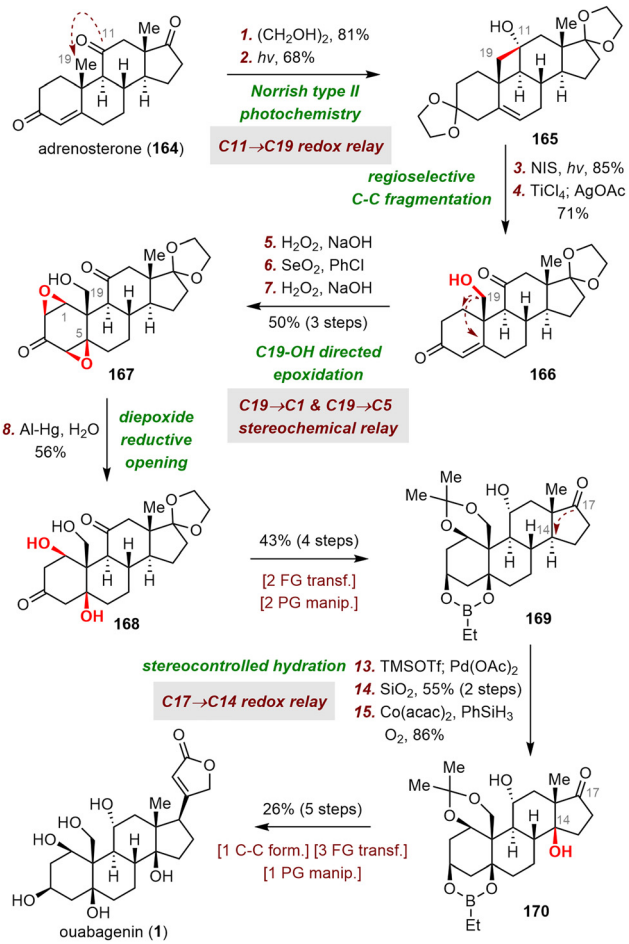

Scheme 27 Baran's synthesis of ouabagenin (**1**).

C5 epoxidation, C1–C2 dehydrogenation, and epoxidation, providing diepoxide **167** in 50% yield from **166**. Reductive opening of the diepoxide using aluminum amalgam generated *in situ* afforded diol **168**, which was advanced to boronic ester **169** in four steps. The final redox relay, from C17 to C14,

Open Access Article. Published on 11 June 2025. Downloaded on 2/11/2026 11:18:29 AM. This article is licensed under a Creative Commons Attribution-NonCommercial 3.0 Unported Licence.

allowed the installation of the C14 hydroxyl group in three steps. Saegusa–Ito oxidation of **169** was followed by double-bond isomerization from C15–C16 to C14–C15 and Mukaiyama hydration to give tertiary alcohol **170**, which was elaborated to ouabagenin (**1**) in five steps.

3.1.2. Zhang's syntheses of clionastatins A and B. In 2022, Zhang and co-workers reported semisyntheses of clionastatins A (**91**) and B (**4**) through a unique two-stage chlorination/oxidation strategy involving a series of redox relays (Scheme 28).[65] The vicinal dichloride unit in the A ring was introduced through a redox relay from the C3 ketone. Specifically, an enone intermediate was obtained by dehydrogenation of **171**, which was followed by reduction of the C3 ketone, protection of the resulting alcohol, and conformationally controlled dichlorination of the C1–C2 double bond to furnish dichloride **172**. Opening of the epoxide of **172** with HBr was followed by C4–OH-directed photochemical C–H oxidation of the C19 methyl group of the resulting bromohydrin intermediate to give tetrahydrofuran intermediate **173**, representing a redox relay from C4 to C19. Intermediate **173** was transformed into trichloride **174** in two steps. Next, a redox relay from the C4–C5 double bond to the C6–C7 double bond was accomplished *via* bromination and dehydrobromination, affording a diene intermediate (not shown) that was converted to ketone **175** *via* deacetylation and oxidation. The C17 ketone in **175** was used as the starting point for installation of the requisite oxidation states at both C15 and C16. Specifically, Saegusa–Ito oxidation of ketone **175**, epoxidation of the resulting enone, and a subsequent Wharton transposition reaction delivered allylic alcohol **176**, which possesses the key C16–C17 double bond of clionastatins A and B. A two-step sequence transformed **176** to dienone **177**, from which clionastatin A (**91**) was obtained *via* desaturation using SeO_2. In this reaction, the C8–C9 double bond was installed by means of a redox relay from the C7 ketone. Moreover, clionastatin B (**4**) was synthesized from intermediate **176** in three steps.

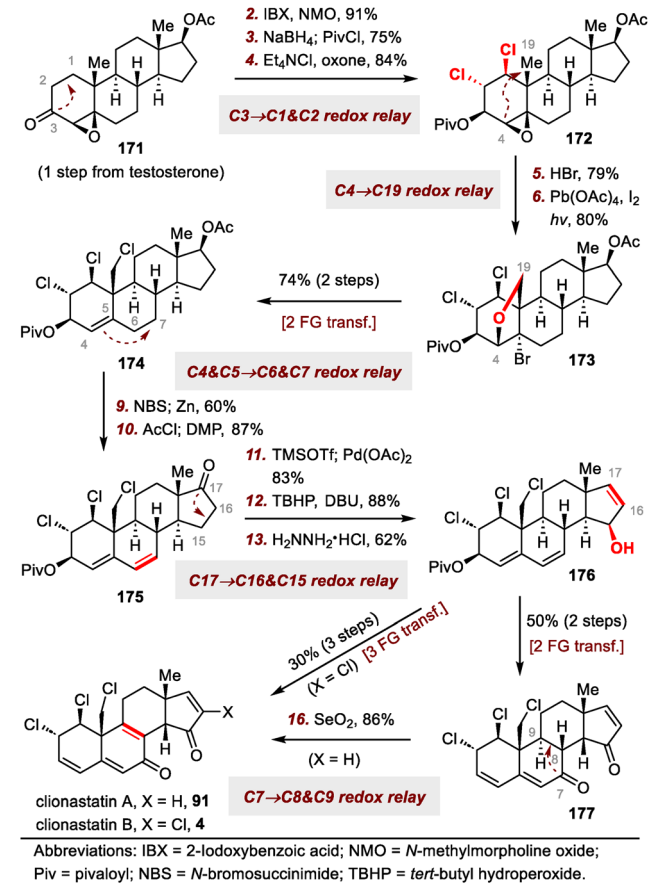

Scheme 28 Zhang's syntheses of clionastatins A (**91**) and B (**4**).

3.2. Skeletal reorganization strategies

Skeletal reorganization of classical steroids, which can be viewed as migration of one or more C–C bonds from one carbon to another within the tetracyclic steroidal skeleton, has emerged as an effective strategy for rapidly accessing the core frameworks of rearranged SNPs, enabling concise, scalable syntheses of these molecules.[17d,20] In this subsection, four molecules have been selected to showcase how the complex core frameworks of rearranged steroids can be rapidly accessed from the tetracyclic skeletons of inexpensive commercially available steroids *via* skeletal reorganization (Scheme 29). In most cases, the proposed biosynthetic pathway of the rearranged steroid proved to be a critical inspiration in realizing the desired skeletal reorganization.[103]

3.2.1. Our group's synthesis of cyclocitrinol. The 5(10 → 19)-*abeo*-steroid cyclocitrinol (**11**), which belongs to the C25 steroid family, possesses an unusual bicyclo[4.4.1]undecane-bridged A/B ring system, and was first isolated by Grafe and co-workers in 2000.[104] So far, more than 30 members of this family have

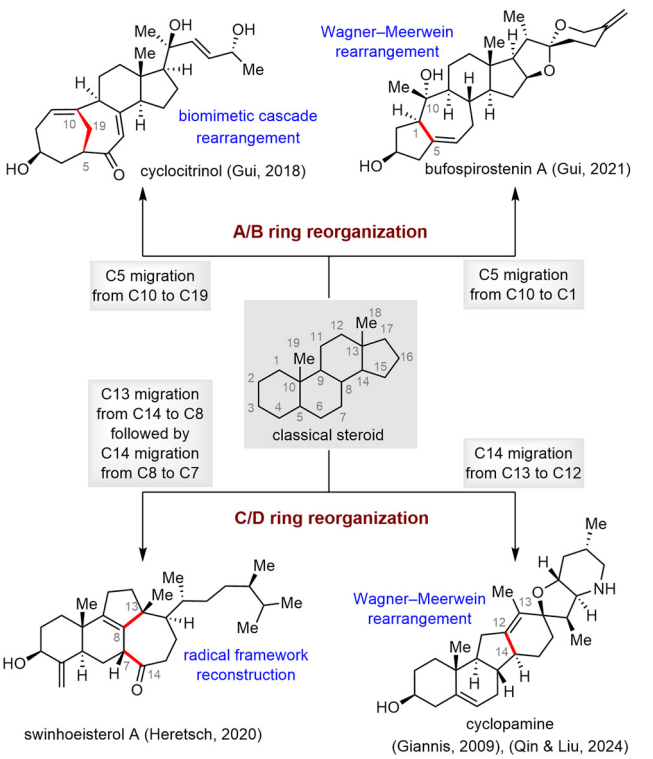

Scheme 29 Skeletal reorganization strategies for synthesis of rearranged steroids.

 This journal is © The Royal Society of Chemistry 2025

Open Access Article. Published on 11 June 2025. Downloaded on 2/11/2026 11:18:29 AM.
This article is licensed under a Creative Commons Attribution-NonCommercial 3.0 Unported Licence.

been isolated, and most of them share the same A/B ring system, therefore offering the opportunity for unified syntheses of these cyclocitrinols. Several cyclocitrinols exhibit promising biological activities, including antibacterial,[105] antiosteoporosis,[105] and antineurotic activities.[106] In 2018, Li and co-workers disclosed the first asymmetric total synthesis of cyclocitrinol, which capitalized on the use of a type II [5+2] cycloaddition strategy to forge the challenging bicyclo[4.4.1]undecane-bridged A/B ring system.[107] Shortly thereafter, our group reported a semisynthetic route to cyclocitrinol based on a bioinspired skeletal reorganization strategy,[108] which ultimately led to the divergent syntheses of ten cyclocitrinols by the same team.[109]

As shown in Scheme 30, heating a solution of allylic sulfoxide **178** in toluene in the presence of *O*-methylquinine as a base effected a *syn*-elimination reaction to give diene **179**. This intermediate underwent cyclopropanation, and a subsequent ring scission reaction of cyclopropylcarbinyl cation **180** generated triene **182** and cycloheptatriene **181**, possibly through regioselective deprotonations at C1 and C9, respectively. This biomimetic cascade rearrangement allowed the construction of the synthetically challenging bridged A/B ring system in only eight steps from commercially available pregnenolone. Moving forward, triene **182**, which has the desired C1–C10 double bond, was elaborated to cyclocitrinol (**11**) in two steps.

3.2.2. Our group's synthesis of bufospirostenin A. The power of the bioinspired skeletal reorganization strategy was also demonstrated in the gram-scale synthesis of bufospirostenin A (**6**) by our group (Scheme 31).[25a] Alcohol **184**, a key intermediate in the synthesis, was prepared in seven steps from known steroidal lactone **183**. Mesylation of **184** and heating of the resulting mesylate **185** at 90 °C in THF/H_2O led to the formation of desired rearranged product **187** in 90% yield. This

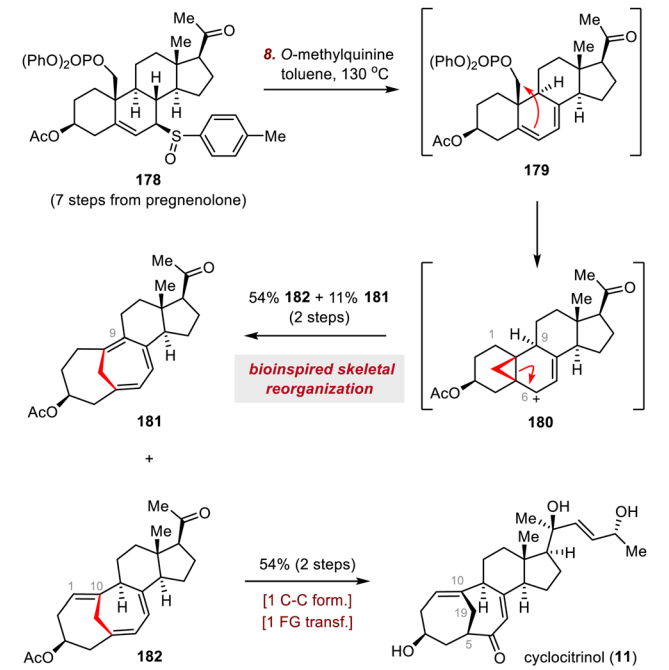

Scheme 30 Our group's synthesis of cyclocitrinol (**11**).

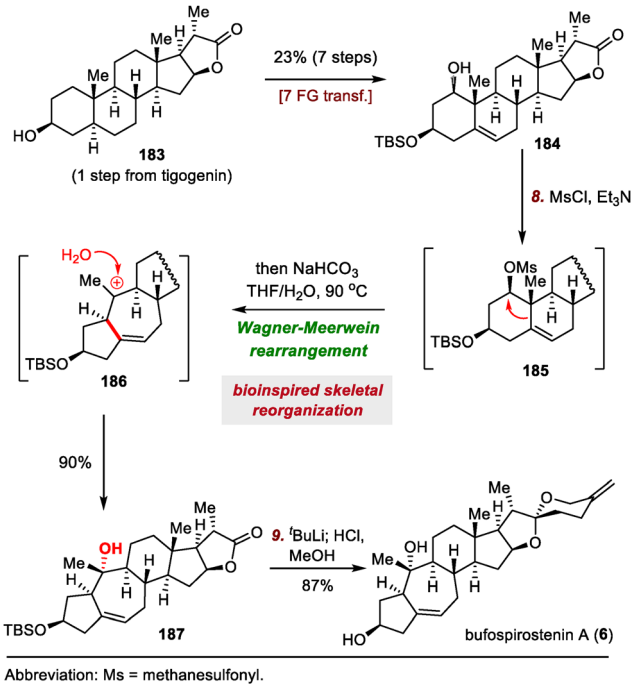

Scheme 31 Our group's synthesis of bufospirostenin A (**6**).

transformation may have proceeded through a Wagner–Meerwein rearrangement of **185** and capture of resulting cationic intermediate **186** by H_2O. Finally, one-step installation of the spiroketal moiety gave bufospirostenin A.

3.2.3. Heretsch's syntheses of swinhoeisterol A, dankasterones A and B, and periconiastone A. A radical cascade–based skeletal reorganization strategy played an important role in the efficient semisyntheses of swinhoeisterol A (**10**), dankasterones A ($\Delta^{4,5}$-**8**) and B (**8**), and periconiastone A (**9**) by Heretsch and co-workers (Scheme 32).[60] The syntheses commenced with a four-step transformation of ergosterol (**188**) to enone **189**. Then two sets of radical conditions to divergently access rearranged steroids **192** and **195** were identified. Specifically, oxidative generation of an alkoxy radical using (diacetoxyiodo)benzene ($PhI(OAc)_2$) and iodine (I_2) led to **190**, which underwent β-scission of the C13–C14 bond followed by a Giese reaction at C8 to give radical intermediate **191**; abstraction of an iodine atom then furnished iodide **192** in 76% yield. Alternatively, upon treatment with HgO/I_2, radical **191** underwent a Dowd–Beckwith rearrangement involving the adjacent C14 ketone, possibly through the intermediacy of **193** and **194**, to produce diketone **195** after loss of a hydrogen atom and desaturation at C9–C11.

A four-step sequence was used to convert iodide **192** to dankasterone B (**8**), from which dankasterone A ($\Delta^{4,5}$-**8**) was accessed *via* a Saegusa–Ito oxidation to desaturate the C4–C5 bond. Alternatively, treatment of dankasterone B with DBU triggered an intramolecular aldol condensation between C4 and C14, affording periconiastone A (**9**) in 86% yield. Swinhoeisterol A (**10**) was synthesized from diketone **195** in seventeen steps, including a series of redox manipulations and installation of the side chain. It is worth noting that, during

Open Access Article. Published on 11 June 2025. Downloaded on 2/11/2026 11:18:29 AM.
This article is licensed under a Creative Commons Attribution-NonCommercial 3.0 Unported Licence.

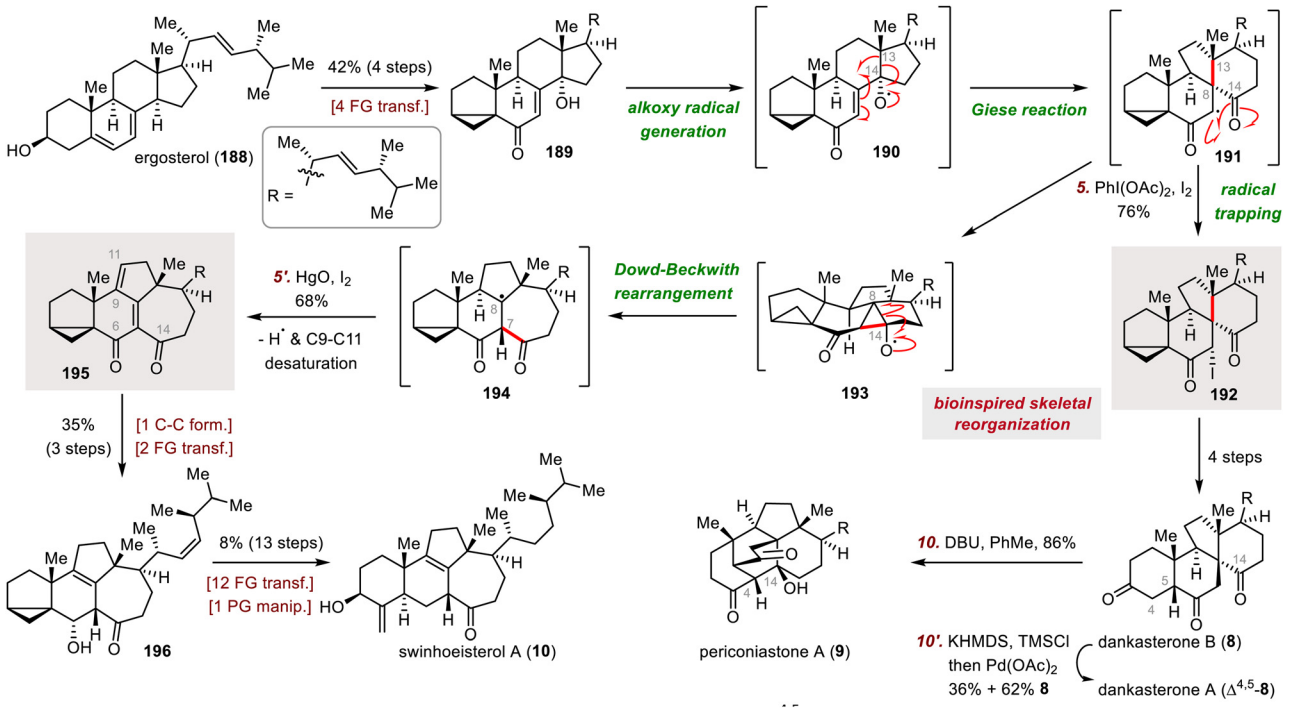

Scheme 32 Heretsch's syntheses of swinhoeisterol A (**10**), dankasterones A ($\Delta^{4,5}$-**8**) and B (**8**), and periconiastone A (**9**).

the revision of this manuscript, our group reported the divergent total syntheses of swinhoeisterols A–C from the Wieland–Miescher ketone. The synthetic strategy involves a tandem Negishi/Heck cross-coupling followed by a Baran reductive olefin coupling to construct the characteristic 5/7-fused ring system.[110]

3.2.4. Giannis's synthesis of cyclopamine. In 2009, Giannis and co-workers reported a semisynthetic route to cyclopamine (**14**) by means of a bioinspired skeletal reorganization strategy (Scheme 33).[91] The synthesis started with a two-step transformation of **197** to **198** *via* Schönecker's directed C–H hydroxylation at C12 and subsequent silylation.[111] Ketone **198** was converted to lactone **199** in three steps, setting the stage for the crucial bioinspired Wagner–Meerwein rearrangement. To this end, desilylation of **199** afforded a secondary alcohol, which reacted with triflic anhydride (Tf_2O) in pyridine at elevated temperature to effect the desired shift of C14 from C13 to C12. This reaction furnished a pair of regioisomeric alkenes in a combined yield of 94% (7 : 3 ratio), with desired *exo* alkene **200** being the major isomer. Alkene **200** was converted to **201** in five steps, and the synthesis of cyclopamine (**14**) was completed in six steps from **201**.

3.2.5. Qin and Liu's syntheses of cyclopamine and veratramine. In 2024, Qin, Liu, and co-workers synthesized cyclopamine (**14**) and veratramine (**13**) on a gram scale by means of a bioinspired skeletal reorganization strategy to build the C-*nor*-D-*homo* skeleton (Scheme 34).[94] A Schönecker C–H hydroxylation,[111] the conditions for which were significantly improved by Baran, Garcia-Bosch, and co-workers,[112] was utilized to synthesize C12 secondary alcohol **203** in three steps from dehydroepiandrosterone (**202**). A two-step transformation of **203** resulted in diol **204**, which

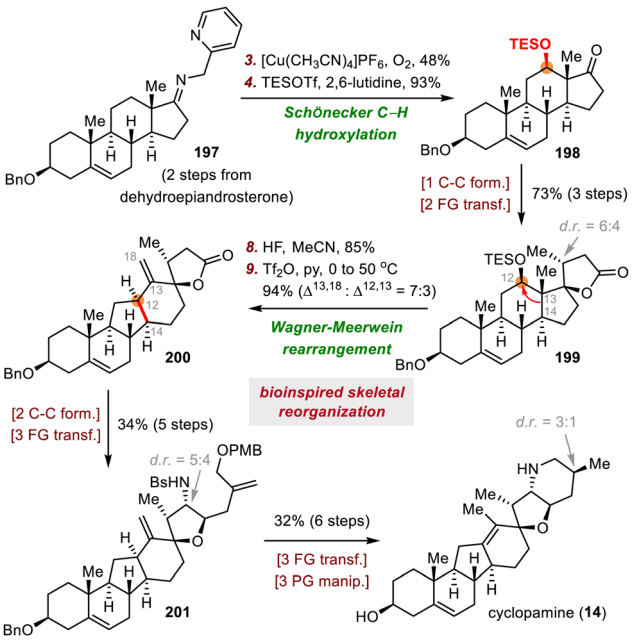

Scheme 33 Giannis's synthesis of cyclopamine (**14**).

served as the starting point for divergent syntheses of cyclopamine and veratramine.

First, treatment of diol **204** with triflic anhydride and 2-chloropyridine initiated the desired Wagner–Meerwein rearrangement, and the resulting C13 carbocation was captured by the adjacent C17 hydroxyl group to give epoxide **205** in 68% yield, along with a 19% yield of alkene **210**. Directed hydrogenation of

 This journal is © The Royal Society of Chemistry 2025

Open Access Article. Published on 11 June 2025. Downloaded on 2/11/2026 11:18:29 AM.
This article is licensed under a Creative Commons Attribution-NonCommercial 3.0 Unported Licence.

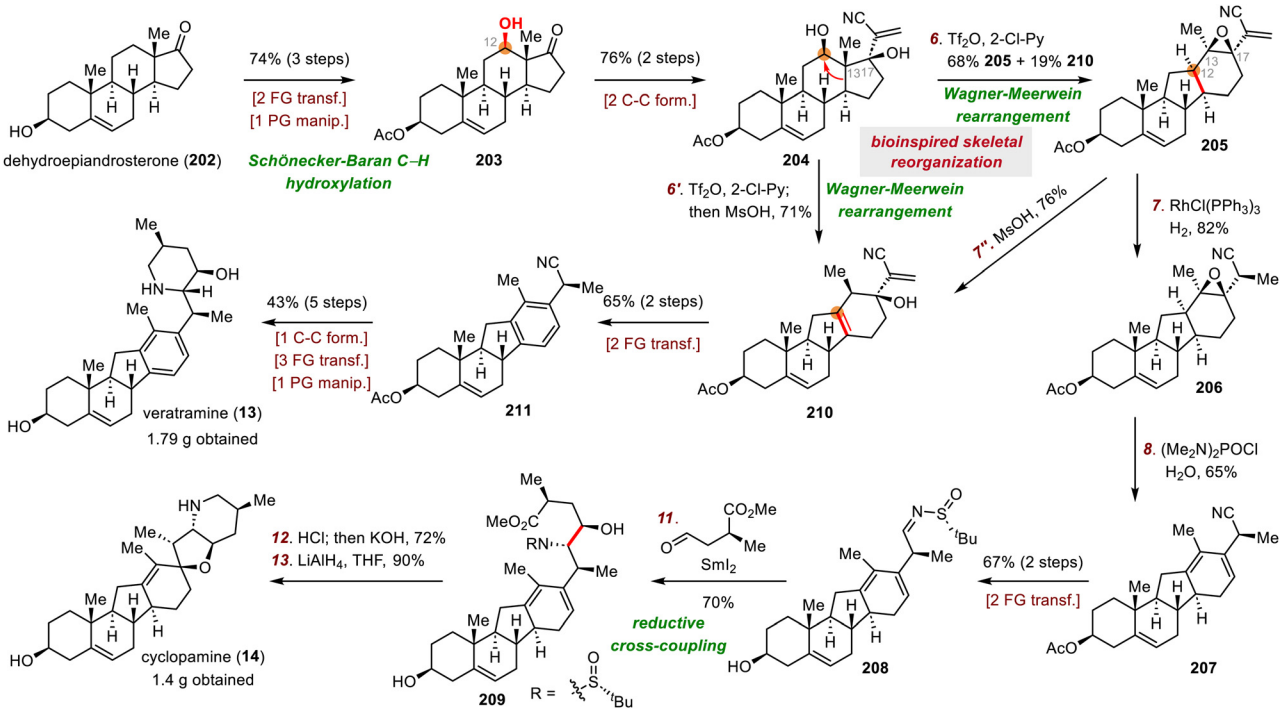

Scheme 34 Qin and Liu's syntheses of cyclopamine (**14**) and veratramine (**13**).

epoxide **205** using Wilkinson's catalyst ($RhCl(PPh_3)_3$) afforded **206** with a dr of 33 : 1. The epoxide was converted to a diene *via* treatment of **206** with $(Me_2N)_2POCl/H_2O$ to give conjugated diene **207** in 65% yield. The cyano group of **207** was converted to a sulfinyl imine (**208**) in two steps, and reductive cross-coupling of **208** with a chiral aldehyde furnished aminoalcohol **209** in 70% yield. Bis-cyclization of **209** using HCl and reduction of the resulting amide with lithium aluminium hydride ($LiAlH_4$) gave cyclopamine (**14**) in two steps.

Second, *in situ* treatment of epoxide **205** with methanesulfonic acid (MsOH) gave thermodynamically stable tetrasubstituted alkene **210**, probably through acid-promoted epoxide opening followed by a 1,2-H shift and deprotonation. Veratramine (**13**) was prepared from **210** in only seven steps. The routes to both **13** and **14** resulted in gram quantities of the target natural products.

4. Conclusion and outlook

The unique and highly functionalized frameworks of SNPs and their intriguing biological activities have rendered these molecules popular targets for both synthetic and medicinal chemists, and significant synthetic and methodological breakthroughs have been achieved. This review has highlighted representative efficient syntheses of SNPs accomplished during the past two decades, grouping the convergent and semisynthetic syntheses on the basis of the key C–C bond forming reactions.

Convergent strategies for SNP synthesis necessitate the rational design of coupling partners, and the coupling and cyclization methods must be judiciously chosen to establish the target polycyclic frameworks. Functionalization of the coupling partners with the maximum number of functional groups minimizes the number of post-coupling redox manipulations. Intramolecular cyclization reactions can be used to build ring systems and install associated stereogenic centers, and synthetic chemists have thus been motivated to invent robust new methodologies. In comparison, semisynthetic strategies for SNP synthesis use known steroids as starting materials, and these strategies typically necessitate a series of redox and stereochemical relays to functionalize the existing C–H bonds, along with skeletal reorganizations to build the rearranged skeletons. For the latter task, biogenetic hypotheses play an important inspirational role in the design of the key cascade transformations. Clearly, both convergent and semisynthetic strategies have their own advantages and disadvantages, and the choice of an appropriate strategy for specific targets largely depends on the synthetic efficiency of each approach, as well as on the opportunities it provides to discover new chemistry.

In recent years, artificial intelligence (AI) techniques have been increasingly applied in the field of chemistry,[113] demonstrating remarkable potential in accelerating the synthesis of complex molecules.[114] Traditionally, the total synthesis of natural products has relied heavily on chemists' specialized knowledge and extensive experimental experience to design retrosynthetic routes—a process that is often time-consuming, labor-intensive, and expensive. In contrast, AI can automatically integrate vast amounts of chemical literature and reaction data into structured databases, enabling the prediction of reaction feasibility and the recommendation of optimal conditions (*e.g.*, temperature, solvents, and catalysts). Clearly, this modern approach streamlines the synthetic planning process by minimizing the need for

Open Access Article. Published on 11 June 2025. Downloaded on 2/11/2026 11:18:29 AM. This article is licensed under a Creative Commons Attribution-NonCommercial 3.0 Unported Licence.

extensive trial-and-error experimentation, thereby significantly reducing experimental costs and enhancing overall efficiency.[114c] One of the most formidable challenges in the synthesis of SNPs lies in the construction of highly oxidized, polycyclic frameworks. By embracing AI-assisted strategies, chemists are now better equipped to address such challenges, making the efficient and scalable synthesis of these structurally intricate molecules increasingly achievable.[115]

In addition, recent years have seen remarkable breakthroughs in enzymatic C–H oxygenation reactions, which exhibit high chemo- and stereoselectivities.[116] Consequently, chemoenzymatic strategies, that is, strategies that combine chemical synthesis with enzymatic C–H oxidation, have become an effective alternative for concise syntheses of bioactive SNPs.[117]

Last but not least, it is important to note that, despite the significant progress made in the synthesis of SNPs, the application of SNP analogs or modified advanced intermediates for biological studies, which is crucial for elucidating detailed structure–activity relationships (SAR) and accelerating drug discovery, still remains in its early stages.[118] This limitation may stem from insufficient interdisciplinary integration. The pursuit of greater efficiency in this exciting field will undoubtedly continue, and we hope this review will further promote the exploration of novel methods and strategies, as well as the development of new steroid drugs in the near future.

Data availability

No primary research results, software or code have been included and no new data were generated or analysed as part of this review.

Conflicts of interest

There are no conflicts to declare.

Acknowledgements

Financial support was provided by the National Key Research and Development Program of China (2021YFF0502400 and 2022YFC2303100), the Talent Plan of Shanghai Branch, Chinese Academy of Sciences (CASSHB-QNPD-2023-009), the Strategic Priority Research Program of the Chinese Academy of Sciences (XDB1060000) and the CAS Project for Young Scientists in Basic Research (YSBR-095). This work has been supported by the New Cornerstone Science Foundation through the XPLORER PRIZE (J. G.).

Notes and references

1 (*a*) D. J. Newman and G. M. Cragg, *J. Nat. Prod.*, 2020, **83**, 770–803; (*b*) K. C. Nicolaou, D. Vourloumis, N. Winssinger and P. S. Baran, *Angew. Chem., Int. Ed.*, 2000, **39**, 44–122; (*c*) S. B. Bharate and C. W. Lindsley, *J. Med. Chem.*, 2024, **67**, 20723–20730.

2 (*a*) D. A. Dias, S. Urban and U. Roessner, *Metabolites*, 2012, **2**, 303–336; (*b*) A. G. Atanasov, S. B. Zotchev, V. M. Dirsch, the International Natural Product Sciences Taskforce and C. T. Supuran, *Nat. Rev. Drug Discovery*, 2021, **20**, 200–216.

3 P. S. Baran, *J. Am. Chem. Soc.*, 2018, **140**, 4751–4755.

4 L. W. Hernandez and D. Sarlah, *Chem. – Eur. J.*, 2019, **25**, 13248–13270.

5 N. A. McGrath, M. Brichacek and J. T. Njardarson, *J. Chem. Educ.*, 2010, **87**, 1348–1349.

6 A. Chaudhuri and D. Anand, *Biomed. Spectrosc. Imaging*, 2017, **6**, 1–24.

7 K. C. Nicolaou and T. Montagnon, *Molecules That Changed the World*, Wiley-VCH, Weinheim, Germany, 2008, pp. 79–90.

8 (*a*) W. S. Johnson, *Acc. Chem. Res.*, 1968, **1**, 1–8; (*b*) W. S. Johnson, *Bioorg. Chem.*, 1976, **5**, 51–98; (*c*) W. S. Johnson, *Angew. Chem., Int. Ed. Engl.*, 1976, **15**, 9–17; (*d*) R. A. Yoder and J. N. Johnston, *Chem. Rev.*, 2005, **105**, 4730–4756.

9 F. Noack, R. C. Heinze and P. Heretsch, *Synthesis*, 2019, 2039–2057.

10 S. Prévost, N. Dupré, M. Leutzsch, Q. Wang, V. Wakchaure and B. List, *Angew. Chem., Int. Ed.*, 2014, **53**, 8770–8773.

11 W. Che, L. Wojitas, C. Shan and J. M. Lopchuk, *Sci. Adv.*, 2024, **10**, eadp9375.

12 K. Cen, J. Bao, X. Wang, H. Tian, Y. Wang and J. Gui, *J. Am. Chem. Soc.*, 2024, **146**, 6481–6486.

13 X. Wang, G. Huang, Y. Wang and J. Gui, *J. Am. Chem. Soc.*, 2023, **145**, 9354–9363.

14 J.-H. Fan, J.-J. Wang, F. Li, G. Wang, Q. Guo, L. W. Chung and C.-C. Li, *CCS Chem.*, 2021, **3**, 348–357.

15 (*a*) J. Xie, X. Liu, N. Zhang, S. Choi and G. Dong, *J. Am. Chem. Soc.*, 2021, **143**, 19311–19316; (*b*) J. Xie, Z. Zheng, X. Liu, N. Zhang, S. Choi, C. He and G. Dong, *J. Am. Chem. Soc.*, 2023, **145**, 4828–4852.

16 A. R. Bucknam and G. C. Micalizio, *J. Am. Chem. Soc.*, 2022, **144**, 8493–8497.

17 (*a*) F. L. Duecker, F. Reuß and P. Heretsch, *Org. Biomol. Chem.*, 2019, **17**, 1624–1633; (*b*) L. Min, L.-P. Zhong and C.-C. Li, *Acc. Chem. Res.*, 2023, **56**, 2378–2390; (*c*) M. Alekseychuk and P. Heretsch, *Chem. Commun.*, 2023, **59**, 6811–6826; (*d*) Y. Wang and J. Gui, *Acc. Chem. Res.*, 2024, **57**, 568–579; (*e*) H. R. Khatri, N. Carney, R. Rutkoski, B. Bhattarai and P. Nagorny, *Eur. J. Org. Chem.*, 2020, 755–776; (*f*) M. T. C. Pessôa, L. A. Barbosa and J. A. F. P. Villar, *Stud. Nat. Prod. Chem.*, 2018, **57**, 79–113; (*g*) P. Gupta and G. Panda, *Eur. J. Org. Chem.*, 2014, 8004–8019; (*h*) M. Kotora, F. Hessler and B. Eignerová, *Eur. J. Org. Chem.*, 2012, 29–42; (*i*) R. Skoda-Földes and L. Kollár, *Chem. Rev.*, 2003, **103**, 4095–4130; (*j*) J. R. Hanson, *Nat. Prod. Rep.*, 2010, **27**, 887–899; (*k*) D. F. Covey, *Steroids*, 2009, **74**, 577–585; (*l*) M. Ibrahim-Ouali and L. Rocheblave, *Steroids*, 2008, **73**, 375–407; (*m*) M. Ibrahim-Ouali and M. Santelli, *Steroids*, 2006, **71**, 1025–1044; (*n*) M. Ibrahim-Ouali, *Steroids*, 2007, **72**, 475–508; (*o*) J.-F. Biellmann, *Chem. Rev.*, 2003, **103**, 2019–2034; (*p*) A.-S. Chapelon, D. Moraléda, R. Rodriguez, C. Ollivier and M. Santelli, *Tetrahedron*, 2007, **63**, 11511–11616.

 This journal is © The Royal Society of Chemistry 2025

Open Access Article. Published on 11 June 2025. Downloaded on 2/11/2026 11:18:29 AM. This article is licensed under a Creative Commons Attribution-NonCommercial 3.0 Unported Licence.

18 (*a*) D. Urabe, T. Asaba and M. Inoue, *Chem. Rev.*, 2015, **115**, 9207–9231; (*b*) Y. Gao and D. Ma, *Acc. Chem. Res.*, 2021, **54**, 569–582.
19 Z. Wang and C. Hui, *Org. Biomol. Chem.*, 2021, **19**, 3791–3812.
20 Z. Zhang, X. Qian, Y. Gu and J. Gui, *Nat. Prod. Rep.*, 2024, **41**, 251–272.
21 Z. G. Brill, M. L. Condakes, C. P. Ting and T. J. Maimone, *Chem. Rev.*, 2017, **117**, 11753–11795.
22 M.-J. Cheng, L.-P. Zhong, C.-C. Gu, X.-J. Zhu, B. Chen, J.-S. Liu, L. Wang, W.-C. Ye and C.-C. Li, *J. Am. Chem. Soc.*, 2020, **142**, 12602–12607.
23 L.-P. Zhong, R. Feng, J.-J. Wang and C.-C. Li, *J. Am. Chem. Soc.*, 2023, **145**, 2098–2103.
24 H.-Y. Tian, L.-J. Ruan, T. Yu, Q.-F. Zheng, N.-H. Chen, R.-B. Wu, X.-Q. Zhang, L. Wang, R.-W. Jiang and W.-C. Ye, *J. Nat. Prod.*, 2017, **80**, 1182–1186.
25 (*a*) Y. Wang, H. Tian and J. Gui, *J. Am. Chem. Soc.*, 2021, **143**, 19576–19586; (*b*) P. Yang, Y.-Y. Li, H. Tian, G.-L. Qian, Y. Wang, X. Hong and J. Gui, *J. Am. Chem. Soc.*, 2022, **144**, 17769–17775.
26 J. Huang, T. Cao, Z. Zhang and Z. Yang, *J. Am. Chem. Soc.*, 2022, **144**, 2479–2483.
27 (*a*) J. Blanco-Urgoiti, L. Añorbe, L. Pérez-Serrano, G. Domínguez and J. Pérez-Castells, *Chem. Soc. Rev.*, 2004, **33**, 32–42; (*b*) Z. Yang, *Acc. Chem. Res.*, 2021, **54**, 556–568.
28 H.-Y. Tian, L. Wang, X.-Q. Zhang, Y. Wang, D.-M. Zhang, R.-W. Jiang, Z. Liu, J.-S. Liu, Y.-L. Li and W.-C. Ye, *Chem. – Eur. J.*, 2010, **16**, 10989–10993.
29 (*a*) P. A. Wender and D. Sperandio, *J. Org. Chem.*, 1998, **63**, 4164–4165; (*b*) B. M. Trost, F. D. Toste and H. Shen, *J. Am. Chem. Soc.*, 2000, **122**, 2379–2380.
30 H. R. El-Seedi, S. A. M. Khalifa, E. A. Taher, M. A. Farag, A. Saeed, M. Gamal, M.-E. F. Hegazy, D. Youssef, S. G. Musharraf, M. M. Alajlani, J. Xiao and T. Efferth, *Pharmacol. Res.*, 2019, **141**, 123–175.
31 C. Mannich and G. Siewert, *Ber. Dtsch. Chem. Ges. A*, 1942, **75**, 737–750.
32 (*a*) H. Renata, Q. Zhou and P. S. Baran, *Science*, 2013, **339**, 59–63; (*b*) H. Renata, Q. Zhou, G. Dünstl, J. Felding, R. R. Merchant, C.-H. Yeh and P. S. Baran, *J. Am. Chem. Soc.*, 2015, **137**, 1330–1340.
33 H. Zhang, M. Sridhar Reddy, S. Phoenix and P. Deslongchamps, *Angew. Chem., Int. Ed.*, 2008, **47**, 1272–1275.
34 K. Mukai, S. Kasuya, Y. Nakagawa, D. Urabe and M. Inoue, *Chem. Sci.*, 2015, **6**, 3383–3387.
35 H. R. Khatri, B. Bhattarai, W. Kaplan, Z. Li, M. J. Curtis Long, Y. Aye and P. Nagorny, *J. Am. Chem. Soc.*, 2019, **141**, 4849–4860.
36 J. Sun, Y. Chen, S. S. Ragab, W. Gu, Z. Tang, Y. Tang and W. Tang, *Angew. Chem., Int. Ed.*, 2023, **62**, e202303639.
37 (*a*) J.-F. Lavallée and P. Deslongchamps, *Tetrahedron Lett.*, 1988, **29**, 6033–6036; (*b*) S. Trudeau and P. Deslongchamps, *J. Org. Chem.*, 2004, **69**, 832–838.
38 N. R. Cichowicz, W. Kaplan, Y. Khomutnyk, B. Bhattarai, Z. Sun and P. Nagorny, *J. Am. Chem. Soc.*, 2015, **137**, 14341–14348.
39 W. Kaplan, H. R. Khatri and P. Nagorny, *J. Am. Chem. Soc.*, 2016, **138**, 7194–7198.
40 B. Bhattarai and P. Nagorny, *Org. Lett.*, 2018, **20**, 154–157.
41 K. Du, P. Guo, Y. Chen, Z. Cao, Z. Wang and W. Tang, *Angew. Chem., Int. Ed.*, 2015, **54**, 3033–3037.
42 (*a*) P. Liu, H. Cheng, T. M. Roberts and J. J. Zhao, *Nat. Rev. Drug Discovery*, 2009, **8**, 627–644; (*b*) J. Yang, J. Nie, X. Ma, Y. Wei, Y. Peng and X. Wei, *Mol. Cancer*, 2019, **18**, 26.
43 (*a*) F. Marra, M. Pinzani, R. DeFranco, G. Laffi and P. Gentilini, *FEBS Lett.*, 1995, **376**, 141–145; (*b*) G. Powis, R. Bonjouklian, M. M. Berggren, A. Gallegos, R. Abraham, C. Ashendel, L. Zalkow, W. F. Matter, J. Dodge, G. Grindey and C. J. Vlahos, *Cancer Res.*, 1994, **54**, 2419–2423; (*c*) P. Wipf and R. J. Halter, *Org. Biomol. Chem.*, 2005, **3**, 2053–2061.
44 (*a*) P. W. Brian, P. J. Curtis, H. G. Hemming and G. F. L. Norris, *Trans. Br. Mycol. Soc.*, 1957, **40**, 365–368; (*b*) T. J. Petcher, H. P. Weber and Z. Kis, *J. Chem. Soc., Chem. Commun.*, 1972, 1061–1062; (*c*) J. MacMillan, T. J. Simpson and S. K. Yeboah, *J. Chem. Soc., Chem. Commun.*, 1972, 1063.
45 (*a*) S. Sato, M. Nakada and M. Shibasaki, *Tetrahedron Lett.*, 1996, **37**, 6141–6144; (*b*) T. Mizutani, S. Honzawa, S.-y Tosaki and M. Shibasaki, *Angew. Chem., Int. Ed.*, 2002, **41**, 4680–4682; (*c*) H. Shigehisa, T. Mizutani, S.-y Tosaki, T. Ohshima and M. Shibasaki, *Tetrahedron*, 2005, **61**, 5057–5065.
46 Y. Guo, T. Quan, Y. Lu and T. Luo, *J. Am. Chem. Soc.*, 2017, **139**, 6815–6818.
47 (*a*) P. W. Brian and J. G. McGowan, *Nature*, 1945, **156**, 144–145; (*b*) J. F. Grove, P. McCloskey and J. S. Moffatt, *J. Chem. Soc. C*, 1966, 743–747.
48 J. S. Moffatt, J. D. Bu'Lock and T. H. Yuen, *J. Chem. Soc. D*, 1969, 839a.
49 (*a*) R. W. Jones and J. G. Hancock, *Can. J. Microbiol.*, 1987, **33**, 963–966; (*b*) G.-A. Pakora, S. Mann, D. M. Kone and D. Buisson, *Bioorg. Chem.*, 2021, **112**, 104959.
50 G.-Q. Wang, G.-D. Chen, S.-Y. Qin, D. Hu, T. Awakawa, S.-Y. Li, J.-M. Lv, C.-X. Wang, X.-S. Yao, I. Abe and H. Gao, *Nat. Commun.*, 2018, **9**, 1838.
51 J. R. Hanson, *Nat. Prod. Rep.*, 1995, **12**, 381–384.
52 E. A. Anderson, E. J. Alexanian and E. J. Sorensen, *Angew. Chem., Int. Ed.*, 2004, **43**, 1998–2001.
53 M. Del Bel, A. R. Abela, J. D. Ng and C. A. Guerrero, *J. Am. Chem. Soc.*, 2017, **139**, 6819–6822.
54 Y. Ji, Z. Xin, H. He and S. Gao, *J. Am. Chem. Soc.*, 2019, **141**, 16208–16212.
55 A. B. Dounay and L. E. Overman, *Chem. Rev.*, 2003, **103**, 2945–2964.
56 (*a*) S. W. M. Crossley, F. Barabé and R. A. Shenvi, *J. Am. Chem. Soc.*, 2014, **136**, 16788–16791; (*b*) S. A. Green, S. W. M. Crossley, J. L. M. Matos, S. Vásquez-Céspedes, S. L. Shevick and R. A. Shenvi, *Acc. Chem. Res.*, 2018, **51**, 2628–2640; (*c*) J. M. Smith, S. J. Harwood and P. S. Baran, *Acc. Chem. Res.*, 2018, **51**, 1807–1817.
57 T. Amagata, M. Doi, M. Tohgo, K. Minoura and A. Numata, *Chem. Commun.*, 1999, 1321–1322.

Open Access Article. Published on 11 June 2025. Downloaded on 2/11/2026 11:18:29 AM. This article is licensed under a Creative Commons Attribution-NonCommercial 3.0 Unported Licence.

58 T. Amagata, M. Tanaka, T. Yamada, M. Doi, K. Minoura, H. Ohishi, T. Yamori and A. Numata, *J. Nat. Prod.*, 2007, **70**, 1731–1740.
59 W. Gao, C. Chai, Y. He, F. Li, X. Hao, F. Cao, L. Gu, J. Liu, Z. Hu and Y. Zhang, *Org. Lett.*, 2019, **21**, 8469–8472.
60 (*a*) F. L. Duecker, R. C. Heinze and P. Heretsch, *J. Am. Chem. Soc.*, 2020, **142**, 104–108; (*b*) F. L. Duecker, R. C. Heinze, S. Steinhauer and P. Heretsch, *Chem. – Eur. J.*, 2020, **26**, 9971–9981.
61 (*a*) P. Chen, C. Wang, R. Yang, H. Xu, J. Wu, H. Jiang, K. Chen and Z. Ma, *Angew. Chem., Int. Ed.*, 2021, **60**, 5512–5518; (*b*) S. Deng, H. Xu, H. Jiang and Z. Ma, *Org. Chem. Front.*, 2022, **9**, 3961–3965.
62 S. W. M. Crossley, C. Obradors, R. M. Martinez and R. A. Shenvi, *Chem. Rev.*, 2016, **116**, 8912–9000.
63 E. Fattorusso, O. Taglialatela-Scafati, F. Petrucci, G. Bavestrello, B. Calcinai, C. Cerrano, P. Di Meglio and A. Ianaro, *Org. Lett.*, 2004, **6**, 1633–1635.
64 W. Ju, X. Wang, H. Tian and J. Gui, *J. Am. Chem. Soc.*, 2021, **143**, 13016–13021.
65 H. Cui, Y. Shen, Y. Chen, R. Wang, H. Wei, P. Fu, X. Lei, H. Wang, R. Bi and Y. Zhang, *J. Am. Chem. Soc.*, 2022, **144**, 8938–8944.
66 (*a*) K. Masuda, M. Nagatomo and M. Inoue, *Nat. Chem.*, 2017, **9**, 207–212; (*b*) D. Kuwana, M. Nagatomo and M. Inoue, *Org. Lett.*, 2019, **21**, 7619–7623; (*c*) H. Fujino, T. Fukuda, M. Nagatomo and M. Inoue, *J. Am. Chem. Soc.*, 2020, **142**, 13227–13234.
67 S. Laschat, F. Narjes and L. E. Overman, *Tetrahedron*, 1994, **50**, 347–358.
68 K. Mukai, D. Urabe, S. Kasuya, N. Aoki and M. Inoue, *Angew. Chem., Int. Ed.*, 2013, **52**, 5300–5304.
69 T. Tokuyama, J. Daly and B. Witkop, *J. Am. Chem. Soc.*, 1969, **91**, 3931–3938.
70 (*a*) N. J. Linford, A. R. Cantrell, Y. Qu, T. Scheuer and W. A. Catterall, *Proc. Natl. Acad. Sci. U. S. A.*, 1998, **95**, 13947–13952; (*b*) S.-Y. Wang, J. Mitchell, D. B. Tikhonov, B. S. Zhorov and G. K. Wang, *Mol. Pharmacol.*, 2006, **69**, 788–795.
71 (*a*) E. X. Albuquerque, J. W. Daly and B. Witkop, *Science*, 1971, **172**, 995–1002; (*b*) G. B. Brown, *Int. Rev. Neurobiol.*, 1988, **29**, 77–116.
72 (*a*) R. Imhof, M. E. Gössinger, W. Graf, H. Berner, M. L. Berner-Fenz and H. Wehrli, *Helv. Chim. Acta*, 1972, **55**, 1151–1153; (*b*) R. Imhof, E. Gössinger, W. Graf, L. Berner-Fenz, H. Berner, R. Schaufelberger and H. Wehrli, *Helv. Chim. Acta*, 1973, **56**, 139–162.
73 M. Kurosu, L. R. Marcin, T. J. Grinsteiner and Y. Kishi, *J. Am. Chem. Soc.*, 1998, **120**, 6627–6628.
74 M. M. Logan, T. Toma, R. Thomas-Tran and J. Du Bois, *Science*, 2016, **354**, 865–869.
75 Y. Guo, Z. Guo, J.-T. Lu, R. Fang, S.-C. Chen and T. Luo, *J. Am. Chem. Soc.*, 2020, **142**, 3675–3679.
76 (*a*) Y. Watanabe, H. Morozumi, H. Mutoh, K. Hagiwara and M. Inoue, *Angew. Chem., Int. Ed.*, 2023, **62**, e202309688; (*b*) Y. Watanabe, K. Sakata, D. Urabe, K. Hagiwara and M. Inoue, *J. Org. Chem.*, 2023, **88**, 17479–17484.
77 D. A. Nicewicz and D. W. C. MacMillan, *Science*, 2008, **322**, 77–80.
78 (*a*) Y. Zhu, L. Zhang and S. Luo, *J. Am. Chem. Soc.*, 2014, **136**, 14642–14645; (*b*) W. Zhang, Y. Zhu, L. Zhang and S. Luo, *Chin. J. Chem.*, 2018, **36**, 716–722.
79 (*a*) J. Uenishi, J. M. Beau, R. W. Armstrong and Y. Kishi, *J. Am. Chem. Soc.*, 1987, **109**, 4756–4758; (*b*) D. Imao, B. W. Glasspoole, V. S. Laberge and C. M. Crudden, *J. Am. Chem. Soc.*, 2009, **131**, 5024–5025.
80 (*a*) S. M. Kupchan, *J. Am. Chem. Soc.*, 1956, **78**, 3546–3547; (*b*) T. J. Gilbertson, *Phytochemistry*, 1973, **12**, 2079–2080.
81 S. M. Kupchan and C. R. Narayanan, *J. Am. Chem. Soc.*, 1959, **81**, 1913–1921.
82 S. M. Kupchan, C. I. Ayres, M. Neeman, R. H. Hensler, T. Masamune and S. Rajagopalan, *J. Am. Chem. Soc.*, 1960, **82**, 2242–2251.
83 (*a*) H.-J. Li, Y. Jiang and P. Li, *Nat. Prod. Rep.*, 2006, **23**, 735–752; (*b*) M. L. Dirks, J. T. Seale, J. M. Collins and O. M. McDougal, *Molecules*, 2021, **26**, 5934.
84 Y. Guo, J.-T. Lu, R. Fang, Y. Jiao, J. Liu and T. Luo, *J. Am. Chem. Soc.*, 2023, **145**, 20202–20207.
85 Y. Guo, R. Fang, Y. Jiao, J. Liu, J.-T. Lu and T. Luo, *Nat. Commun.*, 2024, **15**, 7639.
86 K. Saito, *Bull. Chem. Soc. Jpn.*, 2006, **15**, 22–27.
87 R. F. Keller, *Phytochemistry*, 1968, **7**, 303–306.
88 H.-Y. Kim, S.-W. Lee, S.-K. Choi, J. Ashim, W. Kim, S.-M. Beak, J.-K. Park, J. E. Han, G.-J. Cho, Z. Y. Ryoo, J. Jeong, Y.-H. Lee, H. Jeong, W. Yu and S. Park, *Am. J. Chin. Med.*, 2023, **51**, 1309–1333.
89 M. K. Cooper, J. A. Porter, K. E. Young and P. A. Beachy, *Science*, 1998, **280**, 1603–1607.
90 W. S. Johnson, H. A. P. DeJongh, C. E. Coverdale, J. W. Scott and U. Burckhardt, *J. Am. Chem. Soc.*, 1967, **89**, 4523–4524.
91 (*a*) A. Giannis, P. Heretsch, V. Sarli and A. Stößel, *Angew. Chem., Int. Ed.*, 2009, **48**, 7911–7914; (*b*) P. Heretsch, S. Rabe and A. Giannis, *J. Am. Chem. Soc.*, 2010, **132**, 9968–9969.
92 M. Sofiadis, D. Xu, A. J. Rodriguez, B. Nissl, S. Clementson, N. N. Petersen and P. S. Baran, *J. Am. Chem. Soc.*, 2023, **145**, 21760–21765.
93 H. Shao, W. Liu, M. Liu, H. He, Q.-L. Zhou, S.-F. Zhu and S. Gao, *J. Am. Chem. Soc.*, 2023, **145**, 25086–25092.
94 W. Hou, H. Lin, Y. Wu, C. Li, J. Chen, X.-Y. Liu and Y. Qin, *Nat. Commun.*, 2024, **15**, 5332.
95 M. D. Zott, D. W. Zuschlag and D. H. Trauner, *J. Am. Chem. Soc.*, 2025, **147**, 3010–3016.
96 (*a*) J. K. Crandall and R. P. Haseltine, *J. Am. Chem. Soc.*, 1968, **90**, 6251–6253; (*b*) A. B. Smith and W. C. Agosta, *J. Am. Chem. Soc.*, 1973, **95**, 1961–1968; (*c*) S. Cai, Z. Xiao, Y. Shi and S. Gao, *Chem. – Eur. J.*, 2014, **20**, 8677–8681.
97 Y. Kitamura, M. Nishizawa, K. Kaneko, M. Shiro, Y.-P. Chen and H.-Y. Hsu, *Tetrahedron*, 1989, **45**, 7281–7286.
98 K. J. Cassaidy and V. H. Rawal, *J. Am. Chem. Soc.*, 2021, **143**, 16394–16400.
99 Y. Jin, S. Hok, J. Bacsa and M. Dai, *J. Am. Chem. Soc.*, 2024, **146**, 1825–1831.

 This journal is © The Royal Society of Chemistry 2025

Open Access Article. Published on 11 June 2025. Downloaded on 2/11/2026 11:18:29 AM. This article is licensed under a Creative Commons Attribution-NonCommercial 3.0 Unported Licence.

100 (*a*) H. Gotoh and Y. Hayashi, *Org. Lett.*, 2007, **9**, 2859–2862; (*b*) L. You, X.-T. Liang, L.-M. Xu, Y.-F. Wang, J.-J. Zhang, Q. Su, Y.-H. Li, B. Zhang, S.-L. Yang, J.-H. Chen and Z. Yang, *J. Am. Chem. Soc.*, 2015, **137**, 10120–10123.

101 (*a*) R. Grigg, R. Scott and P. Stevenson, *Tetrahedron Lett.*, 1982, **23**, 2691–2692; (*b*) S. J. Neeson and P. J. Stevenson, *Tetrahedron Lett.*, 1988, **29**, 813–814.

102 B. M. Trost and J. E. Schultz, *Synthesis*, 2019, 1–30.

103 (*a*) R. Bao, H. Zhang and Y. Tang, *Acc. Chem. Res.*, 2021, **54**, 3720–3733; (*b*) L. Chen, P. Chen and Y. Jia, *Acc. Chem. Res.*, 2024, **57**, 3524–3540.

104 A. G. Kozlovsky, V. P. Zhelifonova, V. M. Adanin, S. M. Ozerskaya and U. Grafe, *Pharmazie*, 2000, **55**, 470–471.

105 Z.-H. He, C.-L. Xie, T. Wu, Y.-T. Yue, C.-F. Wang, L. Xu, M.-M. Xie, Y. Zhang, Y.-J. Hao, R. Xu and X.-W. Yang, *J. Nat. Prod.*, 2023, **86**, 157–165.

106 L. Du, T. Zhu, Y. Fang, Q. Gu and W. Zhu, *J. Nat. Prod.*, 2008, **71**, 1343–1351.

107 J. Liu, J. Wu, J.-H. Fan, X. Yan, G. Mei and C.-C. Li, *J. Am. Chem. Soc.*, 2018, **140**, 5365–5369.

108 Y. Wang, W. Ju, H. Tian, W. Tian and J. Gui, *J. Am. Chem. Soc.*, 2018, **140**, 9413–9416.

109 Y. Wang, W. Ju, H. Tian, S. Sun, X. Li, W. Tian and J. Gui, *J. Am. Chem. Soc.*, 2019, **141**, 5021–5033.

110 G. Huang, X. Zhang, Y.-C. Gu and J. Gui, *J. Am. Chem. Soc.*, 2025, **147**, DOI: **10.1021/jacs.5c07053**.

111 B. Schönecker, T. Zheldakova, Y. Liu, M. Kötteritzsch, W. Günther and H. Görls, *Angew. Chem., Int. Ed.*, 2003, **42**, 3240–3244.

112 (*a*) Y. Y. See, A. T. Herrmann, Y. Aihara and P. S. Baran, *J. Am. Chem. Soc.*, 2015, **137**, 13776–13779; (*b*) R. Trammell, Y. Y. See, A. T. Herrmann, N. Xie, D. E. Díaz, M. A. Siegler, P. S. Baran and I. Garcia-Bosch, *J. Org. Chem.*, 2017, **82**, 7887–7904.

113 Z. J. Baum, X. Yu, P. Y. Ayala, Y. Zhao, S. P. Watkins and Q. Zhou, *J. Chem. Inf. Model.*, 2021, **61**, 3197–3212.

114 (*a*) Y. Wang, C. Pang, Y. Wang, J. Jin, J. Zhang, X. Zeng, R. Su, Q. Zou and L. Wei, *Nat. Commun.*, 2023, **14**, 6155; (*b*) Y. Jiang, Y. Yu, M. Kong, Y. Mei, L. Yuan, Z. Huang, K. Kuang, Z. Wang, H. Yao, J. Zou, C. W. Coley and Y. Wei, *Engineering*, 2023, **25**, 32–50; (*c*) R. S. Aal, E. Ali, J. Meng, M. E. I. Khan and X. Jiang, *Artif. Intell. Chem.*, 2024, **2**, 100049; (*d*) F. Strieth-Kalthoff, S. Szymkuć, K. Molga, A. Aspuru-Guzik, F. Glorius and B. A. Grzybowski, *J. Am. Chem. Soc.*, 2024, **146**, 11005–11017; (*e*) D. Meijer, M. A. Beniddir, C. W. Coley, Y. M. Mejri, M. Öztürk, J. J. J. van der Hooft, M. H. Medema and A. Skiredj, *Nat. Prod. Rep.*, 2025, **42**, 654–662; (*f*) Y. Wei, L. Shan, T. Qiu, D. Lu and Z. Liu, *Chin. J. Chem. Eng.*, 2025, **77**, 273–292; (*g*) A. Gangwal and A. Lavecchia, *J. Med. Chem.*, 2025, **68**, 3948–3969.

115 (*a*) Y. Lin, R. Zhang, D. Wang and T. Cernak, *Science*, 2023, **379**, 453–457; (*b*) P. Zhang, J. Eun, M. Elkin, Y. Zhao, R. L. Cantrell and T. R. Newhouse, *Nat. Synth.*, 2023, **2**, 527–534; (*c*) C. Li and R. A. Shenvi, *Nature*, 2025, **638**, 980–986.

116 (*a*) J. Dong, E. Fernández-Fueyo, F. Hollmann, C. E. Paul, M. Pesic, S. Schmidt, Y. Wang, S. Younes and W. Zhang, *Angew. Chem., Int. Ed.*, 2018, **57**, 9238–9261; (*b*) E. King-Smith, C. R. Zwick, III and H. Renata, *Biochemistry*, 2018, **57**, 403–412; (*c*) S. Chakrabarty, Y. Wang, J. C. Perkins and A. R. H. Narayan, *Chem. Soc. Rev.*, 2020, **49**, 8137–8155; (*d*) J. He, K. Yokoi, B. Wixted, B. Zhang, Y. Kawamata, H. Renata and P. S. Baran, *Science*, 2024, **386**, 1421–1427.

117 (*a*) Y. Peng, C. Gao, Z. Zhang, S. Wu, J. Zhao and A. Li, *ACS Catal.*, 2022, **12**, 2907–2914; (*b*) M. Zheng, Z. Lin, S. Lin and X. Qu, *Eur. J. Org. Chem.*, 2024, e202301066; (*c*) H. Song, Z. Zhang, C. Cao, Z. Tang, J. Gui and W. Liu, *Angew. Chem., Int. Ed.*, 2024, **63**, e202319624.

118 (*a*) M. E. Maier, *Org. Biomol. Chem.*, 2015, **13**, 5302–5343; (*b*) B. Hong, T. Luo and X. Lei, *ACS Cent. Sci.*, 2020, **6**, 622–635.